Karlsruhe Institute of Technology

wave phenomena
analysis and numerics

On microlocal artifacts arising in tomography modeled by a class of generalized Radon transforms

Eric Todd Quinto, Andreas Rieder

CRC Preprint 2026/16, May 2026

KARLSRUHE INSTITUTE OF TECHNOLOGY

CRC 1173

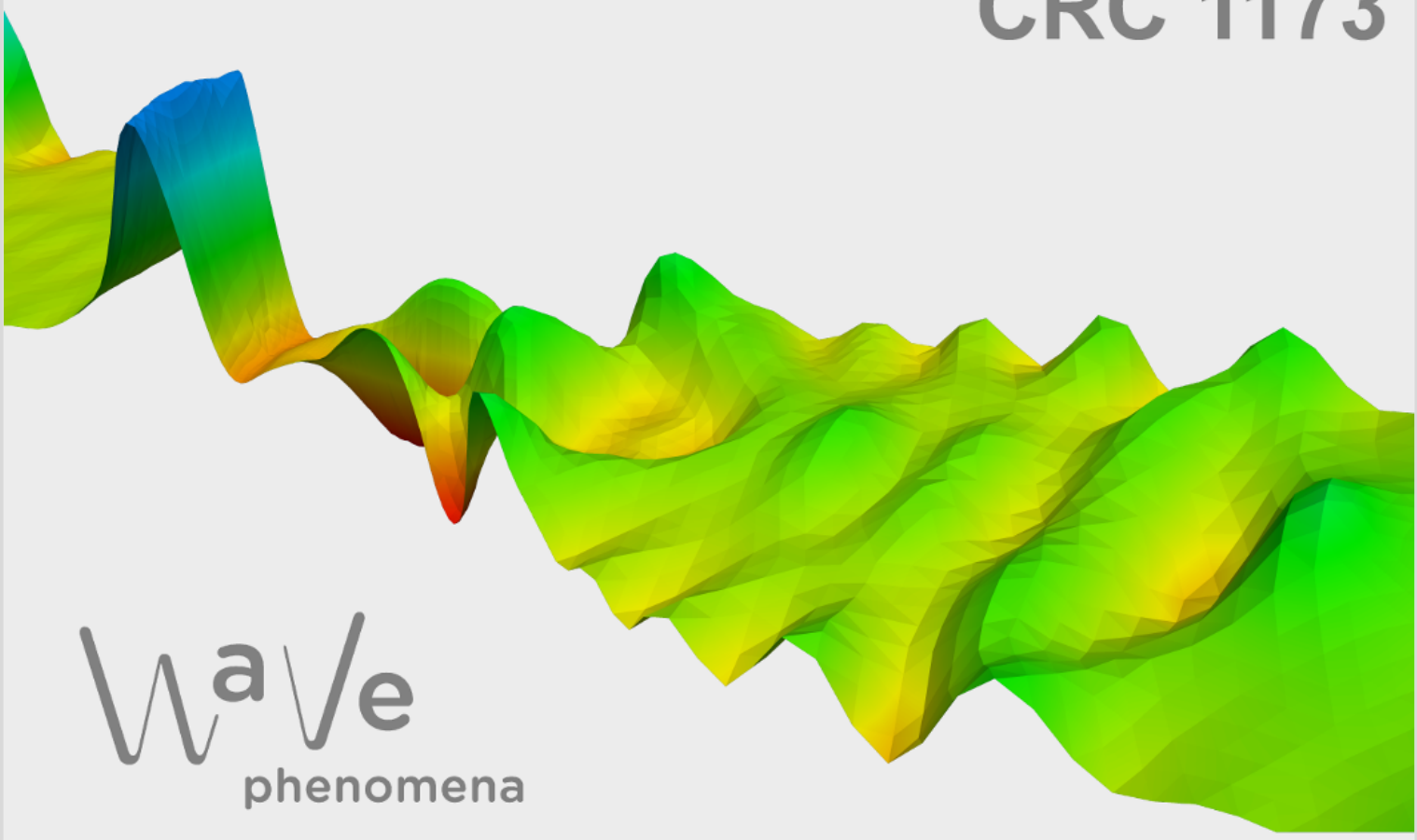

Participating universities

Funded by

ISSN 2365-662X

ON MICROLOCAL ARTIFACTS ARISING IN TOMOGRAPHY MODELED BY A CLASS OF GENERALIZED RADON TRANSFORMS

ERIC TODD QUINTO[1] AND ANDREAS RIEDER[2]

ABSTRACT. In this paper, we provide a unified framework for understanding how and why artifacts arise in limited data tomography, using precise microlocal analysis of the underlying generalized Radon transforms (gRT). Our insights facilitate a more accurate assessment of reconstructions and eventually enable practical artifact reduction strategies in real-world imaging applications. To this end, we consider gRTs as Fourier integral operators whose propagation of singularities is governed by their canonical relations. Thus, we can discern various types of singularities in the reconstructions, including visible singularities (present in both the ground truth and its reconstruction), invisible singularities (present in the ground truth but not in the reconstruction), and artifacts (singularities present in the reconstruction but not in the ground truth). Several concrete examples illustrate the theoretical results: in photoacoustic tomography, mirror artifacts, a special kind of artifacts, arise due a non-injectivity property of the canonical relation (the Bolker condition is violated). In classical X-ray computerized tomography, we consider region of interest (ROI) tomography, where object independent artifacts, a further subtype of artifacts, may manifest at the boundaries of the ROI. Lastly, we investigate artifact formation in linearized seismic imaging (Kirchhoff migration), which depends on the underlying pressure wave velocity model used in the linearization process.

Dedicated to the memory of our good friend and mentor Alfred K. Louis a pioneer and leading researcher in the field who passed away too soon. His legacy continues to guide our work.

1. INTRODUCTION

Generalized Radon transforms (gRT) are models for a broad range of inverse problems. Many problems have limited data; some of the data needed for stable reconstruction are missing. Reconstruction from standard algorithms can generate artifacts, and some parts of the object might not be imaged accurately. In this article, we present a general theory to explain microlocal artifacts in a broad range of tomographic inverse problems and provide formulas to find the artifacts in general.

The transforms we consider are modeled by generalized Radon transforms integrating over hypersurfaces in $\mathbb{R}^n$ that are level sets of a smooth function. Let $\mathtt{S}$ be an open subset of $\mathbb{R}^{n-1}$ or an $n-1$ dimensional smooth manifold such as the sphere, and let X be an open subset of

[1]DEPARTMENT OF MATHEMATICS, TUFTS UNIVERSITY, MEDFORD, MA 02155, USA

[2]DEPARTMENT OF MATHEMATICS, KARLSRUHE INSTITUTE OF TECHNOLOGY (KIT), D-76128 KARLSRUHE, GERMANY

E-mail address: todd.quinto@tufts.edu, andreas.rieder@kit.edu.

Date: May 11, 2026.

2020 *Mathematics Subject Classification.* 35S30, 45Q05, 86A22.

Key words and phrases. generalized Radon transform, limited data tomography, artifact formation, Fourier integral operator.

Funded by the Deutsche Forschungsgemeinschaft (DFG, German Research Foundation) - Project-ID 258734477 - SFB 1173. The first author was partially funded by Simons Foundation grant 708556.

$\mathbb{R}^n$. Let $\varphi\colon \mathtt{S} \times X \to \mathbb{R}$ be a smooth function with nonzero gradient everywhere. For each $(\boldsymbol{s}, t) \in \mathtt{S} \times \mathbb{R}$, the set

$$\mathcal{I}(\boldsymbol{s}, t) = \{\boldsymbol{x} \in \mathbb{R}^n : \ \varphi(\boldsymbol{s}, \boldsymbol{x}) = t\}$$

is an embedded hypersurface in $\mathbb{R}^n$ whenever it is not empty. Our Radon transform

$$Fu(\boldsymbol{s}, t) = \int_{\mathcal{I}(\boldsymbol{s},t)} H(\boldsymbol{s}, \boldsymbol{x})\, u(\boldsymbol{x})\, \mathrm{d}\boldsymbol{x},$$

described in Section 3.1, integrates the function u over the sets $\mathcal{I}(\boldsymbol{s}, t)$ in smooth nowhere zero weight H. Many tomographic inverse problems, such as X-ray tomography, sonar, radar, Compton tomography, and seismic imaging, are modeled by such transforms.

If $A \subsetneq \mathtt{S} \times \mathbb{R}$, then data $Fu(\boldsymbol{s}, t)$ for $(\boldsymbol{s}, t) \in A$ constitute limited data and we study filtered backprojection-type inversion formulas by means of *generalized normal operators*

$$\mathcal{L} = F_W^\dagger \mathbb{1}_A F$$

and variations of it. Here, $\mathbb{1}_A$ is the indicator function of A, and the operator $F_W^\dagger$ denotes a generalized backprojection operator with smooth weight W on $\mathtt{S} \times X$. For instance, if $W = H$ then $F_W^\dagger$ is formal L^2 adjoint. The cutoff $\mathbb{1}_A$ sets the data to zero off of A and provides a simple way to extend the data that is used in practice. There are other ways to extend the data, such as by using the range conditions [30] or an SVD [32], but such extensions are generally highly unstable because the limited data problems are often highly ill-posed. Substituting $\mathbb{1}_A$ with a smooth cutoff has been done, but it can turn microlocal streaks into smoothed streaks and decrease some visible object features (see Remark 3.3).

Our contributions are threefold: First, we provide a general methodology that describes how the limited data imaging operator $\mathcal{L}$ maps singularities or creates artifacts. Second, we present a systematic taxonomy of microlocal artifacts, including object dependent, object independent, and Bolker related artifacts, along with geometric criteria for their occurrence. The latter kind of artifacts emerges when the Bolker condition is violated. This condition is an implicit geometric requirement on φ that ensures a one-to-one, nondegenerate correspondence between the singularities in the ground truth and the reconstructed singularities. Third, we showcase a set of illustrative examples and numerical experiments that demonstrate how the theoretical predictions manifest in practice.

Researchers have studied microlocal artifacts and visible singularities for X-ray CT, starting with [38] and more theoretical articles such as [18] for various X-ray tomography problems. An analysis of the artifacts and visible singularities for limited angle tomography is in [11, 26, 34] and generalized to $\mathbb{R}^n$ in [13]. The article [7] contains a thorough analysis of microlocal artifacts for arbitrary limited data sets for the X-ray transform in $\mathbb{R}^2$. Results for dynamic tomography are in [21], and important results using semiclassical analysis in X-ray CT are in [43] that could be used to analyze limited data problems. A promising statistical 'microlocal' theory is developed in [1]. Machine learning is being used, along with general microlocal principals, to good effect for limited data when one has some a priori information, such as a dictionary of reconstructions [5, 8].

Microlocal analysis is used for many other limited data problems. The spherical transform of photo/thermo acoustic tomography was considered in [12, 35]. This field has been applied to problems in Compton tomography, including in [41] for V-lines, [45] for conical Compton cameras, and [50] for novel Compton scattering tomography problems. The microlocal analysis of artifacts caused by beam-hardening is in [48], and for general nonlinear tomography problems motivated by this in [49].

Our paper is organized as follows. The next section introduces the notation and microlocal tools used in the article: wave front sets, conormal singularities, Fourier integral operators, product results for distributions, and composition rules needed later. Section 3 defines the generalized Radon transform as integration over level sets of a smooth function, represents it as a Fourier integral operator, and describes its canonical relation. It analyzes singularities of $\mathbb{1}_A Fu$ for a distribution u and how they are propagated by the backprojection $F_W^\dagger$. Furthermore, it classifies microlocal singularities and artifacts: visible versus invisible, and artifacts subdivided into Bolker, object independent, and object dependent limited-data artifacts, with precise microlocal criteria for where each arises. Moreover, the section contains theorems stating conditions that prevent or allow certain artifacts, a result on added object independent artifacts when Fu is smooth at the boundary of A, and a characterization of mirror point artifacts when the Bolker condition fails on part of X. Section 4 applies the theory to specific imaging transforms. It first discusses photoacoustic and spherical transforms, explaining microlocal features and mirror-type artifacts, with numerical examples. Next it treats region-of-interest X-ray tomography, identifying visible singularities and limited-data artifacts; numerical experiments show the predicted artifact curves. Finally, Kirchhoff migration in seismic imaging is considered, where straight-line object independent, limited-data, and mirror point artifacts form from the isochrone geometry; numerical reconstructions validate the predictions. The paper ends with appendices containing technical proofs omitted from the main text for easier reading.

2. Microlocal basics

Throughout the article, we will assume that our functions and distributions are real-valued. This is realistic in tomography, and it simplifies certain arguments.

We now provide some standard facts about Fourier integral and pseudodifferential operators as well as observations about wave front sets and singularities that we will use throughout the article. See [23, 36, 46, 47] for full details.

We will let X and Y be open subsets of $\mathbb{R}^n$. Our definitions and terms go over essentially verbatim if $\dim(X) \neq \dim(Y)$, but we do not need this generality (for the Bolker condition given below, $\dim(X)$ must be less than or equal to $\dim(Y)$).

If $B \subset \mathbb{R}^n$ then we let $\dot{B} = B \backslash \{\mathbf{0}\}$.

The standard notation for partial derivatives on $\mathbb{R}^n$ uses multi-indices, $\alpha = (\alpha_1, \dots, \alpha_n) \in (\{0, 1, 2, \dots\})^n$: $D^\alpha f = \frac{\partial^{\alpha_1}}{\partial x_1^{\alpha_1}} \frac{\partial^{\alpha_2}}{\partial x_2^{\alpha_2}} \cdots \frac{\partial^{\alpha_n}}{\partial x_n^{\alpha_n}} f$.

The set $\mathcal{E}(\mathbb{R}^n)$ (or $C^\infty(\mathbb{R}^n)$) is the set of all functions on $\mathbb{R}^n$ that are continuous along with all their derivatives, and $\mathcal{D}(\mathbb{R}^n)$ is the set of all compactly supported functions in $\mathcal{E}(\mathbb{R}^n)$. The Schwartz space, $\mathcal{S}(\mathbb{R}^n)$, is the set of all C^∞ functions on $\mathbb{R}^n$ that rapidly decrease at infinity along with their derivatives. These spaces are all given their standard topologies [42]. Their dual spaces are called distribution spaces and written $\mathcal{D}'(X)$, $\mathcal{E}'(X)$, and $\mathcal{S}'(\mathbb{R}^n)$ respectively, and they are all given the appropriate weak topologies. Note that $\mathcal{E}'(X)$ is the set of distributions of compact support on X,

The geometric concepts we will define, wave front sets and canonical relations, are rigorously defined in terms of cotangent spaces, so we now briefly describe these sets. Let X be an open subset of $\mathbb{R}^n$.

For each $\boldsymbol{x} \in X$, the *tangent space*, $T_{\boldsymbol{x}}(X)$, is the vector space of all first derivatives

$$\boldsymbol{v} = v_1 \frac{\partial}{\partial x_1} + v_2 \frac{\partial}{\partial x_2} + \cdots + v_n \frac{\partial}{\partial x_n}, \tag{1}$$

and by identifying $\boldsymbol{v}$ with the vector $(v_1, \ldots, v_n) \in \mathbb{R}^n$, we can view $T_{\boldsymbol{x}}(X)$ as $\mathbb{R}^n$. The *tangent bundle of* X is the set $T(X) = \{(\boldsymbol{x}, \boldsymbol{v}) : \boldsymbol{x} \in X,\ \boldsymbol{v} \in T_{\boldsymbol{x}}(X)\}$.

For $\boldsymbol{x} \in X$, the *cotangent space*, $T^*_{\boldsymbol{x}}(X)$, is the set of all linear functionals on $T_{\boldsymbol{x}}(X)$. For $j \in \{1, 2, \ldots, n\}$ the linear functional $\mathrm{d}x_j$ is defined $\mathrm{d}x_j \left(\frac{\partial}{\partial x_i}\right) = \delta_{ij}$, the Kronecker delta, and extended linearly, so if $\boldsymbol{v}$ is given in (1), then $\mathrm{d}x_j(\boldsymbol{v}) = v_j$, the j^{th} coordinate of $\boldsymbol{v}$. Similarly, $T^*_{\boldsymbol{x}}(X)$ can be identified this way with $\mathbb{R}^n$ by $(z_1, z_2, \ldots, z_n) \to z_1\,\mathrm{d}x_1 + \cdots + z_n\,\mathrm{d}x_n$.

The *cotangent bundle of* X is $T^*(X) = \{(\boldsymbol{x}, \eta) :\ \boldsymbol{x} \in X,\ \eta \in T^*_{\boldsymbol{x}}(X)\}$.

We let $\dot{T}^*(X) = T^*(X) \backslash (X \times \{\mathbf{0}\})$, the set of nonzero covectors in the cotangent space and if $B \subset X$ then $\dot{T}^*_B(X)$ is the subset $\dot{T}^*(X)$ of cotangent vectors with first coordinate in B.

If $\mathcal{I}$ is a submanifold of $\mathbb{R}^n$, then $N^*(\mathcal{I})$ is the conormal bundle of $\mathcal{I}$, the set of all covectors $(\boldsymbol{x}, \xi)$ such that $\boldsymbol{x} \in \mathcal{I}$ and $T_{\boldsymbol{x}}(\mathcal{I})$ is in the null space of ξ:

$$N^*(\mathcal{I}) = \{(\boldsymbol{x}, \xi) \in T^*(\mathbb{R}^n) :\ \boldsymbol{x} \in \mathcal{I},\ \xi(\boldsymbol{v}) = 0,\ \forall \boldsymbol{v} \in T_{\boldsymbol{x}}(\mathcal{I})\}\,.$$

If $f \colon X \to \mathbb{R}$, then we define

$$\mathrm{d}_{\boldsymbol{x}} f = \frac{\partial f}{\partial x_1}\,\mathrm{d}x_1 + \frac{\partial f}{\partial x_2}\,\mathrm{d}x_2 + \cdots + \frac{\partial f}{\partial x_n}\,\mathrm{d}x_n.$$

Hypersurfaces in $\mathbb{R}^n$ are sets $\mathtt{S}$ that are $n-1$ dimensional embedded manifolds, such as the sphere. Derivatives and the spaces $T(\mathtt{S})$ and $T^*(\mathtt{S})$ are defined using local coordinates.

2.1. **Wave Front Sets and Singularities.** Our first definition provides a precise description of singularity.

Definition 2.1 (Wave front set)**.** *Let $X \subset \mathbb{R}^n$ be open and let $u \in \mathcal{D}'(X)$.*

(a) *u is* microlocally C^∞ *at $(\boldsymbol{x}_0, \xi_0) \in T^*(X)$ if for some $\phi \in \mathcal{D}(X)$ with $\phi(\boldsymbol{x}_0) \neq 0$ and some conic neighborhood V of ξ_0 in $\mathbb{R}^n \backslash \{0\}$, the Fourier transform $\widehat{\phi u}$ is rapidly decaying on V, that is, for every $M \in \mathbb{N}$ exists a constant $C = C(M) > 0$ such that*

$$|\widehat{\phi u}(\xi)| \leq C(1 + |\xi|)^{-M} \quad \textit{for all } \xi \in V.$$

(b) *The* wave front set $\mathrm{WF}(u)$ *of u is the set of all $(\boldsymbol{x}, \xi) \in T^*(X)$ at which u is* not microlocally C^∞ *at $(\boldsymbol{x}, \xi)$.*

If $\boldsymbol{x} \in X$ then we denote the wave front directions above $\boldsymbol{x}$ by

$$\mathrm{WF}_{\boldsymbol{x}}(u) = \{\xi \in T^*_{\boldsymbol{x}} :\ (\boldsymbol{x}, \xi) \in \mathrm{WF}(u)\}\,.$$

If $A \subset X$, then

$$\mathrm{WF}_A(f) = \{(\boldsymbol{x}, \xi) \in \mathrm{WF}(u) :\ \boldsymbol{x} \in A\}\,.$$

As noted, we will often assume functions and distributions are real-valued. This allows us to use the following fact.

Proposition 2.2. *If u is a real-valued locally integrable function or real-valued distribution and $(\boldsymbol{x}, \xi) \in \mathrm{WF}(u)$, then $(\boldsymbol{x}, \omega\xi) \in \mathrm{WF}(u)$ for all $\omega \in \dot{\mathbb{R}}$.*

This proposition is true for locally integrable functions because, if φ is a smooth real-valued cutoff function, then $\mathcal{F}(\varphi u)(-\xi) = \overline{\mathcal{F}(\varphi u)(\xi)}$ since u is real-valued. Thus, $\mathcal{F}(\varphi u)$ rapidly decays in direction ξ if and only if $\mathcal{F}(\varphi u)$ rapidly decays in direction $-\xi$. The conclusion follows from the fact that wave front sets are conic. The proof for real-valued distributions is similar.

In general, one cannot multiply distributions, but our next theorem provides conditions in which one can.

Theorem 2.3 (Products of Distributions [24, Theorem 8.2.10])**.** *Let u and v be distributions on an open set X. Assume the* non-cancellation condition

$$\forall(\boldsymbol{x},\xi)\in T^*(X),\quad \textit{if}\ \ (\boldsymbol{x},\xi)\in \mathrm{WF}(u),\quad \textit{then}\ \ (\boldsymbol{x},-\xi)\notin \mathrm{WF}(v). \tag{2}$$

Then the product uv is a distribution on X and

$$\mathrm{WF}(uv)\subset\{(\boldsymbol{x},\xi+\eta):\ (\boldsymbol{x},\xi)\in\mathrm{WF}(u)\ (\boldsymbol{x},\eta)\in\mathrm{WF}(v)\}\cup\mathrm{WF}(u)\cup\mathrm{WF}(v) \tag{3}$$

Remark 2.4. *If v is smooth at $\boldsymbol{x}$, then there is no η such that $(\boldsymbol{x},\eta)\in\mathrm{WF}(v)$. In this case, we interpret $(\boldsymbol{x},\xi+\eta)$ in (3) to mean $(\boldsymbol{x},\xi)$, and similarly if u is smooth at $\boldsymbol{x}$. Thus, some covectors in $\mathrm{WF}(u)$ and $\mathrm{WF}(v)$ are double-counted, but that does not make a difference to the result.*

Also, for real-valued distributions or locally integrable functions, the condition (2) can be written, $\mathrm{WF}(u)\cap\mathrm{WF}(v)=\emptyset$ since, for real-valued distributions, $(\boldsymbol{x},-\xi)\in\mathrm{WF}(v)$ if and only if $(\boldsymbol{x},\xi)\in\mathrm{WF}(v)$. The proof is a direct application of Proposition 2.2.

If u and v are bounded locally integrable functions, then uv is always a distribution, but the non-cancellation condition might not hold. Our next corollary provides a local version of Theorem 2.3 and includes results for functions when a local non-cancellation condition fails. We will use this corollary in analyzing singularities and artifacts in Section 3.

Corollary 2.5 (Local Properties of Products)**.** *Let u and v be bounded, real-valued locally integrable functions, and let $\boldsymbol{x}_0\in X$.*

(i) *If v is smooth near $\boldsymbol{x}_0$, then*

$$\mathrm{WF}_{\boldsymbol{x}_0}(uv)\subset\mathrm{WF}_{\boldsymbol{x}_0}(u). \tag{4}$$

If $v(\boldsymbol{x}_0)\neq 0$, then equality holds in (4).

(ii) *If the following* local non-cancellation condition holds *above $\boldsymbol{x}_0$,*

$$\forall\xi\in T^*_{\boldsymbol{x}_0}(X),\quad \textit{if}\ \ \xi\in\mathrm{WF}_{\boldsymbol{x}_0}(u)\quad \textit{then}\quad -\xi\notin\mathrm{WF}_{\boldsymbol{x}_0}(v), \tag{5}$$

then

$$\mathrm{WF}_{\boldsymbol{x}_0}(uv)\subset\{\xi+\eta:\ \xi\in\mathrm{WF}_{\boldsymbol{x}_0}(u)\ \eta\in\mathrm{WF}_{\boldsymbol{x}_0}(v)\}\cup\mathrm{WF}_{\boldsymbol{x}_0}(u)\cup\mathrm{WF}_{\boldsymbol{x}_0}(v) \tag{6}$$

(iii) *Let u and v be real-valued functions. Then the local non-cancellation condition holds above $\boldsymbol{x}_0$, if and only if*

$$\mathrm{WF}_{\boldsymbol{x}_0}(u)\cap\mathrm{WF}_{\boldsymbol{x}_0}(v)=\emptyset. \tag{7}$$

Equivalently, if $\xi\in\mathrm{WF}_{\boldsymbol{x}_0}(u)$ and $\eta\in\mathrm{WF}_{\boldsymbol{x}_0}(v)$, then ξ and η are linearly independent.

Statement (ii) follows from applying Theorem 2.3 to localized versions of u and v (if $\xi\in\mathrm{WF}_{\boldsymbol{x}_0}(u)$ but not in $\mathrm{WF}_{\boldsymbol{x}_0}(v)$, then there is a cutoff at $\boldsymbol{x}_0$, φ, such that the same is true for φu and φv). Statement (iii) follows from Proposition 2.2. The proofs of the other statements are left to the reader.

2.2. **Fourier integral operators.**

Fourier integral operators (FIO) are defined in terms of phase functions and symbols, and we give the basic definitions as found in [23, 25].

Definition 2.6 (Phase function)**.** *A real-valued function $\Phi\in\mathcal{E}(Y\times X\times\mathbb{R}^N\backslash\{\mathbf{0}\})$ with arguments $(\boldsymbol{y},\boldsymbol{x},\xi)$ is called a* phase function *if it is positively homogeneous of degree 1 in ξ and $(\mathrm{d}_{\boldsymbol{y}}\Phi,\mathrm{d}_\xi\Phi)$ as well as $(\mathrm{d}_{\boldsymbol{x}}\Phi,\mathrm{d}_\xi\Phi)$ do not vanish on $Y\times X\times\mathbb{R}^N\backslash\{\mathbf{0}\}$.*

The phase function is nondegenerate *if the set* $\{\mathrm{d}_{(\boldsymbol{y},\boldsymbol{x},\xi)}\partial_{\xi_j}\Phi : j = 1,\dots,N\}$ *is linearly independent on the manifold*

$$\Sigma_\Phi = \big\{(\boldsymbol{y},\boldsymbol{x},\xi) \in Y \times X \times \mathbb{R}^N\backslash\{\mathbf{0}\} : \mathrm{d}_\xi\Phi(\boldsymbol{y},\boldsymbol{x},\xi) = 0\big\}.$$

Definition 2.7 (Symbol)**.** *A function* $p \in \mathcal{E}(Y \times X \times \mathbb{R}^N\backslash\{\mathbf{0}\})$ *is a* symbol of order $m \in \mathbb{R}$ *if for every compact set* $\mathrm{K} \subset Y \times X$ *and all multi-indices* $\alpha \in \mathbb{N}_0^N$, $\beta \in \mathbb{N}_0^d$, *and* $\gamma \in \mathbb{N}_0^d$ *there exists a positive constant* $C = C(\mathrm{K},\alpha,\beta,\gamma)$ *such that*

$$|D_\xi^\alpha D_{\boldsymbol{x}}^\beta D_{\boldsymbol{y}}^\gamma p(\boldsymbol{y},\boldsymbol{x},\xi)| \le C(1+|\xi|)^{m-|\alpha|}$$

holds for all $(\boldsymbol{y},\boldsymbol{x}) \in \mathrm{K}$ *and all* ξ *with* $|\xi| \ge 1$. *The set of all symbols of order* m *is denoted by* $S^m(Y \times X \times \mathbb{R}^N)$.

If $p \in S^m(Y \times X \times \mathbb{R}^N)$, *then* p *is* elliptic of order m *(or* elliptic *if the order is clear) if, for each compact subset* K *of* $Y \times X$, *there are positive constants* c *and* M *such that*

$$|p(\boldsymbol{y},\boldsymbol{x},\xi)| \ge c\,(1+|\xi|)^m \tag{8}$$

for all $(\boldsymbol{y},\boldsymbol{x}) \in \mathrm{K}$ *and all* ξ *with* $|\xi| \ge M$.

Definition 2.8 (Fourier integral operator)**.** *Given a symbol* $p \in S^m(Y \times X \times \mathbb{R}^N\backslash\{\mathbf{0}\})$ *and a nondegenerate phase function* $\Phi \in \mathcal{E}(Y \times X \times \mathbb{R}^N\backslash\{\mathbf{0}\})$ *we define the* Fourier integral operator *(FIO)* F *applied to* $u \in \mathcal{D}(X)$ *by*

$$Fu(\boldsymbol{y}) = \int_{\mathbb{R}^N}\int_X p(\boldsymbol{y},\boldsymbol{x},\xi)u(\boldsymbol{x})\mathrm{e}^{\imath\Phi(\boldsymbol{y},\boldsymbol{x},\xi)}\,\mathrm{d}\boldsymbol{x}\,\mathrm{d}\xi \tag{9}$$

The order *of the operator* F *is* $k := m - \left(\frac{n-N}{2}\right)$.

If F is an FIO, then (9) is called an oscillatory integral and F maps $\mathcal{D}(X)$ continuously to $\mathcal{E}(Y)$ and can be extended as a continuous map from $\mathcal{E}'(X)$ to $\mathcal{D}'(Y)$, see [23, Chap. I].

Definition 2.9. *If* F *is an FIO with phase function* $\Phi \in \mathcal{E}(Y \times X \times \mathbb{R}^N)$, *then the* canonical relation of F *is the set*

$$\mathcal{C} = \big\{\big(\boldsymbol{y}, \mathrm{d}_{\boldsymbol{y}}\Phi(\boldsymbol{y},\boldsymbol{x},\xi); \boldsymbol{x}, -\mathrm{d}_{\boldsymbol{x}}\Phi(\boldsymbol{y},\boldsymbol{x},\xi)\big) : (\boldsymbol{y},\boldsymbol{x},\xi) \in \Sigma_\Phi\big\} \subset T^*(Y) \times T^*(X).$$

The transpose, $\mathcal{C}^\top$ *of* $\mathcal{C}$ *is obtained from* $\mathcal{C}$ *by switching the* $T^*(Y)$ *and* $T^*(X)$ *coordinates of* $\mathcal{C}$.

The canonical relation, $\mathcal{C}$, of an FIO F encodes how F propagates singularities, see (11) below. To this end, we denote the canonical left projection from $\mathcal{C}$ to $T^*(Y)$ by $\Pi_{\mathrm{L}}\colon \mathcal{C} \to T^*(Y)$, and the canonical right projection by $\Pi_{\mathrm{R}}\colon \mathcal{C} \to T^*(X)$. If $W \subset T^*(X)$ then the composition with $\mathcal{C}$ is defined

$$\mathcal{C} \circ W = \{(\boldsymbol{s},t,\eta) : \exists(\boldsymbol{x},\xi) \in W,\ (\boldsymbol{s},t,\eta;\boldsymbol{x},\xi) \in \mathcal{C}\} \tag{10}$$

Then, for $u \in \mathcal{E}'(X)$,

$$\begin{aligned}\mathrm{WF}(Fu) \subset \mathcal{C} \circ \mathrm{WF}(u) &= \Pi_{\mathrm{L}}\Pi_{\mathrm{R}}^{-1}\left(\mathrm{WF}(u)\right)\\ &= \{(\boldsymbol{y},\eta) \in T^*(Y) : \exists(\boldsymbol{x},\xi) \in \mathrm{WF}(u)\colon (\boldsymbol{y},\eta;\boldsymbol{x},\xi) \in \mathcal{C}\}.\end{aligned} \tag{11}$$

The inclusion (11) is called the *Hörmander-Sato lemma*, see [24, Theorem 8.2.13].

Definition 2.10 (The Bolker condition [19, 20])**.** *Let* $F\colon \mathcal{E}'(X) \to \mathcal{D}'(Y)$ *be an FIO and let* $\mathcal{C}$ *be its canonical relation. Then* F *(or* $\mathcal{C}$*) satisfies the* Bolker condition *if*

$$\Pi_{\mathrm{L}}\colon \mathcal{C} \to T^*(Y) \text{ is an injective immersion.} \tag{12}$$

If an FIO F satisfies the Bolker condition, then it has important microlocal properties. Let F^* be the formal L^2 adjoint of F. Assume that F^*F is well defined. Then, under the Bolker condition, F^*F is a pseudodifferential operator, see [20].

Pseudodifferential operators (ΨDO) are FIOs where $X = Y \subset \mathbb{R}^n$ and $\Phi(\boldsymbol{y}, \boldsymbol{x}, \xi) = (\boldsymbol{y}-\boldsymbol{x})\cdot \xi$ is the nondegenerate phase function. Their canonical relation is Δ, the diagonal in $\dot{T}^*(X)^2$.

Pseudodifferential operators are FIOs with favorable qualities for imaging. For instance, they do not create singularities:

$$\mathrm{WF}(Pu) \subset \mathrm{WF}(u) \quad \text{for any } u \in \mathcal{E}'(X).$$

In case P is elliptic (i.e., its symbol is elliptic), equality holds [36, p. 226]:

$$\mathrm{WF}(Pu) = \mathrm{WF}(u) \quad \text{for any } u \in \mathcal{E}'(X).$$

3. Limited Data Imaging Operators

In this section, we outline the general techniques we will use to analyze artifacts. We remind readers that we will consider only real-valued functions.

3.1. The forward operator and backprojection.

First, we describe our Radon transform and the sets that define it in a fairly general setting. We will follow this notation throughout the article.

We let X be an open subset of $\mathbb{R}^n$ and let $\mathtt{S}$ be a smooth hypersurface in $\mathbb{R}^n$, such as the unit sphere, or an open subset of $\mathbb{R}^{n-1}$. When $\mathtt{S}$ is an embedded manifold in $\mathbb{R}^n$, then we will understand $\mathrm{d}_{\boldsymbol{s}}\varphi$ as the differential of φ on $\mathtt{S}$, and when needed, we will calculate it using local coordinates.

Let $\varphi\colon \mathtt{S} \times X \to \mathbb{R}$ be a smooth function. Assume

$$\forall (\boldsymbol{s}, \boldsymbol{x}) \in \mathtt{S} \times X, \quad \mathrm{d}_{\boldsymbol{x}}\varphi(\boldsymbol{s}, \boldsymbol{x}) \neq \mathbf{0}. \tag{13}$$

Let $Y = \mathtt{S} \times \mathbb{R}$.

Our Radon transform will integrate over level sets of the smooth function φ:

$$\mathcal{I}(\boldsymbol{s}, t) = \{\boldsymbol{x} \in X : \ \varphi(\boldsymbol{s}, \boldsymbol{x}) = t\}, \quad (\boldsymbol{s}, t) \in Y. \tag{14}$$

Note that (13) ensures $\mathcal{I}(\boldsymbol{s}, t)$ is an embedded hypersurface in X whenever $\mathcal{I}(\boldsymbol{s}, t)$ is nonempty.

Let $H \in \mathcal{E}(\mathtt{S} \times X)$ be nowhere zero, and define the *Generalized Radon Transform* (GRT) of $u \in \mathcal{E}'(X)$ to be

$$Fu(\boldsymbol{s}, t) = \int_X H(\boldsymbol{s}, \boldsymbol{x}) u(\boldsymbol{x})\, \delta(t - \varphi(\boldsymbol{s}, \boldsymbol{x}))\, \mathrm{d}\boldsymbol{x}. \tag{15}$$

As proven in [15], using the Fourier representation for the delta function, F is an FIO

$$Fu(\boldsymbol{s}, t) = \frac{1}{2\pi} \int_X \int_{\mathbb{R}} H(\boldsymbol{s}, \boldsymbol{x}) u(\boldsymbol{x}) \mathrm{e}^{\imath \Phi(\boldsymbol{s}, t, \boldsymbol{x}, \omega)}\, \mathrm{d}\omega\, \mathrm{d}\boldsymbol{x} \tag{16}$$

with nondegenerate phase function

$$\Phi(\boldsymbol{s}, t, \boldsymbol{x}, \omega) = \omega(t - \varphi(\boldsymbol{s}, \boldsymbol{x})) \tag{17}$$

and canonical relation

$$\mathcal{C} = \left\{ (\boldsymbol{s}, t, -\omega\, \mathrm{d}_{\boldsymbol{s}}\varphi(\boldsymbol{s}, \boldsymbol{x}), \omega; \boldsymbol{x}, \omega\, \mathrm{d}_{\boldsymbol{x}}\varphi(\boldsymbol{s}, \boldsymbol{x})) : \ (\boldsymbol{s}, t, \omega) \in Y \times \dot{\mathbb{R}}, \boldsymbol{x} \in \mathcal{I}(\boldsymbol{s}, t) \right\}. \tag{18}$$

Note that

$$\mathtt{S} \times X \times \dot{\mathbb{R}} \ni (\boldsymbol{s}, \boldsymbol{x}, \omega) \mapsto (\boldsymbol{s}, \varphi(\boldsymbol{s}, \boldsymbol{x}), -\omega\, \mathrm{d}_{\boldsymbol{s}}\varphi, \omega; \boldsymbol{x}, \omega\, \mathrm{d}_{\boldsymbol{x}}\varphi) \tag{19}$$

give global coordinates on $\mathcal{C}$.

Let $D \subset Y$. We define

$$\mathcal{C}_D = \{(\boldsymbol{s}, t, \eta; \boldsymbol{x}, \xi) \in \mathcal{C} : \ (\boldsymbol{s}, t) \in D\}. \tag{20}$$

This is the set of points in $\mathcal{C}$ whose first coordinates are in D.

Let W be a smooth nowhere zero real-valued weight on $\mathtt{S} \times X$. Then, we define the *generalized backprojection* $F_W^\dagger \colon \mathcal{E}'(Y) \to \mathcal{D}'(X)$ by

$$F_W^\dagger g(\boldsymbol{x}) = \int_{\mathtt{S}} g(\boldsymbol{s}, \varphi(\boldsymbol{s}, \boldsymbol{x}))W(\boldsymbol{s}, \boldsymbol{x}) \, \mathrm{d}\boldsymbol{s}.$$

The formal L^2-adjoint F^* has weight $W = H$. Using similar arguments, $F_W^\dagger$ is an FIO with a nondegenerate phase function

$$F_W^\dagger g(\boldsymbol{x}) = \int_Y \int_{\mathbb{R}} \mathrm{e}^{i\Phi(\boldsymbol{s},t,\boldsymbol{x},\omega)} g(\boldsymbol{x}, t)W(\boldsymbol{s}, \boldsymbol{x}) \, \mathrm{d}\omega \, \mathrm{d}\boldsymbol{s} \, \mathrm{d}t, \tag{21}$$

and $F_W^\dagger$ is a generalized dual or backprojection operator to F. The canonical relation of $F_W^\dagger$ is $\mathcal{C}^\top$, see [23]. It is also worth pointing out that our theorems will be valid for any Radon transform defined by φ with a smooth, nowhere zero real-valued weight on F since they are elliptic FIOs with the same microlocal properties as F.

3.2. **The limited data operator.** Many of the most interesting inverse problems have limited data–not all data needed for standard reconstruction methods is available. We now describe one fairly standard way of dealing with limited data.

Definition 3.1 (Limited Data Set)**.** *A set $A \subset Y$ will be a* limited data set *if $A \neq Y$ and A is connected, compact, and has nontrivial interior. To exclude degenerate cases, we assume $A = \mathrm{Cl}(\mathrm{Int}(A))$.*

If F is the forward operator, then the limited data (forward) operator *is $\mathbb{1}_A F$.*

Note that $\operatorname{sing\,supp}(\mathbb{1}_A) = \mathrm{Bd}(A)$ since $A = \mathrm{Cl}(\mathrm{Int}(A))$.

The limited data operator just takes the given data on A and extends it by zero to all of Y. Researchers often use standard reconstruction methods on this extended data.

If u is an arbitrary distribution, then $\mathbb{1}_A Fu$ might not be defined if the non-cancellation condition (2) fails. However, if u is a bounded measurable function of compact support, then Fu is a locally bounded measurable function, so $\mathbb{1}_A Fu$ is a distribution, and we can use Corollary 2.5 to calculate a superset for $\mathrm{WF}(\mathbb{1}_A Fu)$. This superset, which sometimes even coincides with $\mathrm{WF}(\mathbb{1}_A Fu)$, will be calculated in Section 3.6.

Remark 3.2. *If F is properly supported, that is, $F \colon \mathcal{E}'(X) \to \mathcal{E}'(Y)$, then A does not need to be compact, as long as A is connected and closed, and $A = \mathrm{Cl}(\mathrm{Int}(A))$. This is true since in this case, $B = A \cap \operatorname{supp}(Fu)$ will be compact for every $u \in \mathcal{E}'(X)$.*

For a smooth nowhere zero weight W on $\mathtt{S} \times X$ we will consider the *generalized normal operator*

$$\mathcal{L} = F_W^\dagger \mathbb{1}_A F. \tag{22}$$

Let P and Q be properly supported ΨDO's. More general operators can be formed as follows

$$P F_W^\dagger Q \mathbb{1}_A F. \tag{23}$$

Because A is compact and P and Q are properly supported, the compositions all are defined for $u \in \mathcal{E}'(X)$. If $P = 1$ and Q is an elliptic properly supported ΨDO, then $F_W^\dagger Q \mathbb{1}_A F$ is a *generalized filtered backprojection operator*. These operators have the same microlocal

properties as $\mathcal{L}$, except they can be of different orders depending on the order of P and Q. This type of operator covers concrete examples in the literature (see, e.g., [7, 15, 26, 34]).

Remark 3.3. *We mention two reasons to consider smooth cutoffs rather than $\mathbb{1}_A$.*

When data are not limited, the operators in (22) and (23) are defined but without the $\mathbb{1}_A$. However, if F^* cannot be composed with F, then one uses a compactly supported smooth cutoff, $\phi\colon Y \to \mathbb{R}$, and forms the operator $F^*\phi F$, or in the more general case, $PF_W^\dagger Q\phi F$. We will use this convention without comment when needed.

In limited data tomography, one way to suppress the artifacts caused by multiplication with $\mathbb{1}_A$ is to replace $\mathbb{1}_A$ by a smooth cutoff function $\phi\colon Y \to [0,1]$ that is supported in A. Then, our general operator becomes $KF_W^\dagger \phi LF$. Multiplying by the smooth function ϕ does not add non-smooth artifacts to Fu. However, smoothed versions of the artifacts still appear, unless one makes ϕ close to zero on a large enough subset of A to smooth out some of the visible singularities that are near the artifacts. This is shown by example in [29].

In addition, many researchers use the sharp cutoff $\mathbb{1}_A$ because it is simple and natural when extending the data so they can implement standard reconstruction methods, such as the normal operator or filtered backprojection inversion formulas, on the limited data.

Therefore, understanding the artifacts we consider is important even if one uses a smooth cutoff ϕ instead of $\mathbb{1}_A$.

Unless otherwise noted, we will assume u is in $L^1_c(X,\mathbb{R})$, the set of all real-valued integrable functions of compact support in X.

3.3. **Singularities of $\mathbb{1}_A Fu$.** To analyze singularities of $\mathcal{L}u$, we first analyze singularities of $\mathbb{1}_A Fu$. We will use these results to find possible singularities of $\mathcal{L}u$.

The more intricate proofs will be in the appendix, in particular, those involving composition with $\mathcal{C}_A$ or $\mathcal{C}_A^\top$, but we will provide an overview of the process and more straightforward justifications here.

To simplify our expressions, we define the following set. For $(\boldsymbol{s},t) \in Y$ and $u \in L^1_c(X,\mathbb{R})$, let

$$\mathcal{X}(\boldsymbol{s},t,u) = \{\boldsymbol{x}_0 \in \mathcal{I}(\boldsymbol{s},t) : \ (\boldsymbol{x}_0,\ \mathrm{d}_{\boldsymbol{x}}\varphi(\boldsymbol{s},\boldsymbol{x}_0)) \in \mathrm{WF}(u)\}\,. \tag{24}$$

As justified by Proposition A.1, the set $\mathcal{X}(\boldsymbol{s},t,u)$ contains the base points of all covectors in $N^*(\mathcal{I}(\boldsymbol{s},t)) \cap \mathrm{WF}(u)$ and

$$\boldsymbol{x}_0 \in \mathcal{X}(\boldsymbol{s},t,u) \implies \forall \omega \in \dot{\mathbb{R}},\ (\boldsymbol{s},t,-\omega\,\mathrm{d}_{\boldsymbol{s}}\varphi(\boldsymbol{s},\boldsymbol{x}_0),\omega) \in \mathcal{C}\circ\mathrm{WF}(u). \tag{25}$$

The implication

$$(\boldsymbol{s},t,\eta) \in \mathcal{C}\circ\mathrm{WF}(u) \implies \exists \boldsymbol{x}_0 \in \mathcal{X}(\boldsymbol{s},t,u),\ \omega \in \dot{\mathbb{R}},\ \eta = (-\omega\,\mathrm{d}_{\boldsymbol{s}}\varphi(\boldsymbol{s},\boldsymbol{x}_0),\omega) \tag{26}$$

follows from (58) in Proposition A.1.

We will use $\mathcal{X}(\boldsymbol{s},t,u)$ as an upper bound for base points in X that generate singularities in Fu since every singularity of Fu is in $\mathcal{C}\circ\mathrm{WF}(u)$ (by the Hörmander-Sato lemma) and every singularity in $\mathcal{C}\circ\mathrm{WF}(u)$ above $(\boldsymbol{s},t)$ can be generated by a singularity above some $\boldsymbol{x}_0 \in \mathcal{X}(\boldsymbol{s},t,u)$ by (26).

Since we assume F is elliptic, if $F\colon \mathcal{E}'(X) \to \mathcal{D}'(Y)$ satisfies the Bolker condition (12), then $\mathcal{C}\circ\mathrm{WF}(u) = \mathrm{WF}(Fu)$, so in this case,

$$\boldsymbol{x}_0 \in \mathcal{X}(\boldsymbol{s},t,u) \iff \forall \omega \in \dot{\mathbb{R}}, (\boldsymbol{s},t,-\omega\,\mathrm{d}_{\boldsymbol{s}}\varphi(\boldsymbol{s},\boldsymbol{x}_0),\omega) \in \mathrm{WF}(Fu). \tag{27}$$

For $\eta = (\eta_1,\eta_2,\ldots,\eta_n) \in \mathbb{R}^n$ set $\eta' = (\eta_1,\eta_2,\ldots,\eta_{n-1})$.

We will use the following result several places in our calculations. Let $D \subset Y$. Then,

$$\begin{aligned} \mathrm{WF}_D(Fu) \subset \mathcal{C}_D \circ \mathrm{WF}(u) = & \bigcup_{\substack{(\boldsymbol{s},t)\in D \\ \mathcal{X}(\boldsymbol{s},t,u)\neq\emptyset}} \left\{(\boldsymbol{s},t,-\omega\, \mathrm{d}_{\boldsymbol{s}}\varphi(\boldsymbol{s},\boldsymbol{x}_0),\omega) :\ \boldsymbol{x}_0 \in \mathcal{X}(\boldsymbol{s},t,u),\right. \\ & \left. \omega \in \dot{\mathbb{R}}\right\} \qquad (28) \\ =: & M^{\mathrm{F}}(D,u). \end{aligned}$$

This calculation is verified in Proposition B.1. If $F\colon \mathcal{E}'(X) \to \mathcal{D}'(Y)$ satisfies the Bolker condition (12), then, by (27),

$$\mathrm{WF}_D(Fu) = M^{\mathrm{F}}(D,u). \qquad (29)$$

We will now describe the different microlocal singularities that can appear in $\mathbb{1}_A Fu$. The only singularities of $\mathbb{1}_A Fu$ are above A. We first consider singularities of $\mathbb{1}_A Fu$ above $\mathrm{Int}(A)$ and then consider the more subtle case of singularities above $\mathrm{Bd}(A)$.

Singularities of $\mathbb{1}_A Fu$ *above* $\mathrm{Int}(A)$. Since the function $\mathbb{1}_A$ is smooth and nonzero on $\mathrm{Int}(A)$, the singularities of $\mathbb{1}_A Fu$ above $\mathrm{Int}(A)$ are those of Fu. We now calculate these singularities in terms of $\mathrm{WF}(u)$. From (28), we see that

$$\mathrm{WF}_{\mathrm{Int}(A)}(\mathbb{1}_A Fu) = \mathrm{WF}_{\mathrm{Int}(A)}(Fu) \subset M^{\mathrm{F}}(\mathrm{Int}(A),u). \qquad (30)$$

Singularities of $\mathbb{1}_A Fu$ *above* $\mathrm{Bd}(A)$. To analyze the interaction of singularities of $\mathbb{1}_A$ with those of Fu, we will use Corollary 2.5, which describes the wave front sets of products. With this in mind, we define the following sets:

$$\begin{aligned} B &= \mathrm{Bd}(A) \cap \mathrm{supp}(Fu), \\ B_2 &= \mathrm{Bd}(A) \cap \mathrm{sing\,supp}(Fu), \\ B_2^{\mathrm{c}} &= \left\{(\boldsymbol{s},t) \in B_2 :\ \mathrm{WF}_{(\boldsymbol{s},t)}(\mathbb{1}_A) \cap \mathrm{WF}_{(\boldsymbol{s},t)}(Fu) \neq \emptyset\right\}, \\ B_2^{\mathrm{nc}} &= \left\{(\boldsymbol{s},t) \in B_2 :\ \mathrm{WF}_{(\boldsymbol{s},t)}(\mathbb{1}_A) \cap \mathrm{WF}_{(\boldsymbol{s},t)}(Fu) = \emptyset\right\}. \end{aligned} \qquad (31)$$

Since $\mathrm{Bd}(A) = \mathrm{sing\,supp}(\mathbb{1}_A)$, B is the largest subset of $\mathrm{Bd}(A)$ on which $\mathbb{1}_A Fu$ can have a singularity. Note that

$$B_2 = \mathrm{sing\,supp}(\mathbb{1}_A) \cap \mathrm{sing\,supp}(Fu) = B_2^{\mathrm{c}} \cup B_2^{\mathrm{nc}}$$

is the set of points above which *both* $\mathbb{1}_A$ and Fu have singularities.

The non-cancellation condition of Corollary 2.5 part (ii) fails if $(\boldsymbol{s},t) \in B_2^{\mathrm{c}}$ by part (iii) of that corollary. The superscript 'c' stands for *cancellation*. The non-cancellation condition holds if $(\boldsymbol{s},t) \in B_2^{\mathrm{nc}}$ by Corollary 2.5 part (iii), hence 'nc' for *non-cancellation*. We will analyze these cases separately.

First, assume the local non-cancellation condition (5) fails at $(\boldsymbol{s},t)$. This is equivalent to $(\boldsymbol{s},t) \in B_2^{\mathrm{c}}$. Since we cannot use Corollary 2.5 part (ii) above $(\boldsymbol{s},t)$, we will take the largest set of possible singularities of the function $\mathbb{1}_A Fu$ above $(\boldsymbol{s},t)$, which is $\dot{T}^*_{(\boldsymbol{s},t)}(Y)$, because $\mathrm{WF}_{(\boldsymbol{s},t)}(\mathbb{1}_A Fu)$ is always a subset of $T^*_{(\boldsymbol{s},t)}(Y)$. The set of all such possible singularities is

$$T^*_{B_2^{\mathrm{c}}}(Y) = \left\{(\boldsymbol{s},t,\eta) \in \dot{T}^*(Y) :\ (\boldsymbol{s},t) \in B_2^{\mathrm{c}}\right\} \qquad (32)$$

$$\begin{aligned} \subset & \bigcup_{(\boldsymbol{s},t)\in A} \left\{(\boldsymbol{s},t,\eta) \in \dot{T}^*(Y) :\ \exists \boldsymbol{x}_0 \in \mathcal{X}(\boldsymbol{s},t,u),\right. \\ & \left. (\boldsymbol{s},t,-\mathrm{d}_{\boldsymbol{s}}\varphi(\boldsymbol{s},\boldsymbol{x}_0),1) \in \mathrm{WF}(\mathbb{1}_A)\right\} \qquad (33) \\ =: & M^{\mathrm{c}}(A,u). \end{aligned}$$

If one knows B_2^{c}, then one should use equation (32) in (36) as an upper bound for $\mathrm{WF}(\mathbb{1}_A Fu)$, and if not, one can use (33).

The set $M^{\mathrm{c}}(A,u)$ will be our upper bound for the set of singularities of $\mathbb{1}_A Fu$ above points at which the local non-cancellation condition (5) could fail (when B_2^{c} is not known). The containment in (32)-(33) will be justified in Proposition B.2.

If $F\colon \mathcal{E}'(X) \to \mathcal{D}'(Y)$ satisfies the Bolker condition (12), then $T^*_{B_2^{\mathrm{c}}}(Y) = M^{\mathrm{c}}(A,u)$ by (27).

Now, consider the other case, when the local non-cancellation condition (5) holds, i.e., when $(\boldsymbol{s},t) \in B_2^{\mathrm{nc}}$. In this case, the set of possible added singularities are sums of covectors in the respective wave front sets:

$$\begin{aligned}\big\{(\boldsymbol{s},t,&\eta+\nu) \in \dot{T}^*(Y) :\ (\boldsymbol{s},t) \in B_2^{\mathrm{nc}}, \eta \in \mathrm{WF}_{(\boldsymbol{s},t)}(\mathbb{1}_A),\ \nu \in \mathrm{WF}_{(\boldsymbol{s},t)}(Fu)\big\} \qquad (34)\\
&\subset \bigcup_{(\boldsymbol{s},t)\in B_2^{\mathrm{nc}}} \big\{(\boldsymbol{s},t,\eta+\nu) \in \dot{T}^*(Y) :\ \eta \in \mathrm{WF}_{(\boldsymbol{s},t)}(\mathbb{1}_A),\ \omega \in \dot{\mathbb{R}},\\
&\qquad\qquad \boldsymbol{x}_0 \in \mathcal{X}(\boldsymbol{s},t,u),\ :\ \nu = (-\omega\, \mathrm{d}_{\boldsymbol{s}}\varphi(\boldsymbol{s},\boldsymbol{x}_0),\omega)\big\} \qquad (35)\\
&=: M^{\mathrm{nc}}(A,u).\end{aligned}$$

This is justified in Proposition B.3.

Note that one needs to know B_2^{nc} to use these expressions. In the appendix, we provide a superset of B_2^{nc}, see (67), that can be used in place of B_2^{nc}, if B_2^{nc} is not known.

If both B_2^{nc} and $\mathrm{WF}(Fu)$ are known, one can use (34) in place of $M^{\mathrm{nc}}(A,u)$ in (36). However, if $\mathrm{WF}(Fu)$ has not been calculated, then $M^{\mathrm{nc}}(A,u)$ provides an upper bound for the set of singularities of $\mathbb{1}_A Fu$ above points at which the local non-cancellation condition (5) holds.

The only other singularities that affect the product $\mathbb{1}_A Fu$ are the last two sets in (6),

$$\mathrm{WF}_{B_2}(\mathbb{1}_A) \cup \mathrm{WF}_{B_2}(Fu)$$

union the separate singularities of $\mathbb{1}_A$ and of Fu above $B \setminus B_2$, in all: $\mathrm{WF}_B(\mathbb{1}_A) \cup \mathrm{WF}_B(Fu)$, which we will deal with in (36).

Summary. Putting this all together, we see that

$$\begin{aligned}\mathrm{WF}(\mathbb{1}_A Fu) &\subset \mathrm{WF}_{\mathrm{Int}(A)}(\mathbb{1}_A Fu) \cup M^{\mathrm{c}}(A,u) \cup M^{\mathrm{nc}}(A,u) \cup \mathrm{WF}_B(\mathbb{1}_A) \cup \mathrm{WF}_B(Fu)\\
&\subset M^{\mathrm{F}}(A,u) \cup M^{\mathrm{c}}(A,u) \cup M^{\mathrm{nc}}(A,u) \cup \mathrm{WF}_{\mathrm{supp}(Fu)}(\mathbb{1}_A)\end{aligned} \qquad (36)$$

where we used that $B \subset \mathrm{supp}(Fu)$ so $\mathrm{WF}_B(\mathbb{1}_A) = \mathrm{WF}_{\mathrm{supp}(Fu)}(\mathbb{1}_A)$ and then that

$$\mathrm{WF}_{\mathrm{Int}(A)}(\mathbb{1}_A Fu) = \mathrm{WF}_{\mathrm{Int}(A)}(Fu)$$

and, by (28),

$$\mathrm{WF}_{\mathrm{Int}(A)}(Fu) \cup \mathrm{WF}_{\mathrm{Bd}(A)}(Fu) = \mathrm{WF}_A(Fu) \subset M^{\mathrm{F}}(A,u).$$

3.4. **Singularities of $F^*\mathbb{1}_A Fu = \mathcal{L}u$.** We now analyze the singularities that can occur when reconstructing using the limited data operator $\mathcal{L}$ in (22). Our analysis is valid for the more general operators given by (23).

We will first provide the general formulas and, in subsequent sections, apply these results to transforms with specific microlocal properties.

Let u be a real-valued integrable function of compact support. We estimate $\mathrm{WF}(\mathcal{L}u)$ using the Hörmander-Sato lemma (11) on the terms in (36), and this becomes

$$\begin{aligned}\mathrm{WF}(\mathcal{L}u) \subset &\left(\mathcal{C}_A^\top \circ M^{\mathrm{F}}(A,u)\right) \cup \left(\mathcal{C}_A^\top \circ M^{\mathrm{c}}(A,u)\right) \cup \left(\mathcal{C}_A^\top \circ M^{\mathrm{nc}}(A,u)\right)\\
&\cup \left(\mathcal{C}_A^\top \circ \mathrm{WF}_{\mathrm{supp}(Fu)}(\mathbb{1}_A)\right).\end{aligned} \qquad (37)$$

We now use the expression for $\mathcal{C}_A$ in (18) and the definition of $\mathcal{C}_A^\top$ to give each of the four terms in (37). The proofs are in Section B.

The first composition in (37) is

$$\mathcal{C}_A^\top \circ M^{\mathrm{F}}(A,u) = \bigcup_{\substack{(\boldsymbol{s},t)\in A\\ \mathcal{X}(\boldsymbol{s},t,u)\neq\emptyset}} \big\{(\boldsymbol{x}, \omega\, \mathrm{d}_{\boldsymbol{x}}\varphi(\boldsymbol{s},\boldsymbol{x})) :\ \boldsymbol{x}\in\mathcal{I}(\boldsymbol{s},t),\ \omega\in\dot{\mathbb{R}},\ \boldsymbol{x}_0\in\mathcal{X}(\boldsymbol{s},t,u),\ \mathrm{d}_{\boldsymbol{s}}\varphi(\boldsymbol{s},\boldsymbol{x}) = \mathrm{d}_{\boldsymbol{s}}\varphi(\boldsymbol{s},\boldsymbol{x}_0)\big\}. \tag{38}$$

as will be justified in Proposition C.1.

The second composition in (37) is

$$\mathcal{C}_A^\top \circ T^*_{B_2^{\mathrm{c}}}(Y) = \bigcup_{(\boldsymbol{s},t)\in B_2^{\mathrm{c}}} \dot{N}^*(\mathcal{I}(\boldsymbol{s},t)), \tag{39}$$

and this set is contained in

$$\mathcal{C}_A^\top \circ M^{\mathrm{c}}(A,u) = \bigcup_{(\boldsymbol{s},t)\in A} \big\{(\boldsymbol{x},\xi)\in\dot{N}^*(\mathcal{I}(\boldsymbol{s},t)) :\ \exists \boldsymbol{x}_0\in\mathcal{X}(\boldsymbol{s},t,u),\ (\boldsymbol{s},t,-\mathrm{d}_{\boldsymbol{s}}\varphi(\boldsymbol{s},\boldsymbol{x}_0),1)\in \mathrm{WF}(\mathbb{1}_A)\big\}. \tag{40}$$

The set (39) is the union of all $\dot{N}^*(\mathcal{I}(\boldsymbol{s},t))$ for which u has a singularity conormal to $\mathcal{I}(\boldsymbol{s},t)$ that produces a singularity in $\mathrm{WF}_{(\boldsymbol{s},t)}(Fu)$ that is also in $\mathrm{WF}_{(\boldsymbol{s},t)}(\mathbb{1}_A)$. This is justified in Proposition C.2. This suggests that artifacts can be smeared over all of $\mathcal{I}(\boldsymbol{s},t)$ for such $(\boldsymbol{s},t)$.

If one knows B_2^{c}, then one should use equation (39) in (37), and if not, one can use (40). If $F\colon \mathcal{E}'(X)\to\mathcal{D}'(Y)$ satisfies the Bolker condition, then these sets are equal.

The third composition in (37) is

$$\mathcal{C}_A^\top \circ M^{\mathrm{nc}}(A,u) = \bigcup_{(\boldsymbol{s},t)\in B_2^{\mathrm{nc}}} \big\{(\boldsymbol{x}, (\eta_n+\omega)\, \mathrm{d}_{\boldsymbol{x}}\varphi(\boldsymbol{s},\boldsymbol{x})) :\ \eta\in\mathrm{WF}_{(\boldsymbol{s},t)}(\mathbb{1}_A),\ \omega\in\dot{\mathbb{R}},\ \eta_n+\omega\neq 0,\ \boldsymbol{x}\in\mathcal{I}(\boldsymbol{s},t), \exists \boldsymbol{x}_0\in\mathcal{X}(\boldsymbol{s},t,u),\ \mathrm{d}_{\boldsymbol{s}}\varphi(\boldsymbol{s},\boldsymbol{x}) = \frac{1}{\eta_n+\omega}(\omega\, \mathrm{d}_{\boldsymbol{s}}\varphi(\boldsymbol{s},\boldsymbol{x}_0)-\eta')\big\}. \tag{41}$$

This is justified in Proposition C.3.

Next, we give the last set in (37):

$$\mathcal{C}_A^\top \circ \mathrm{WF}_{\mathrm{supp}(Fu)}(\mathbb{1}_A) = \big\{(\boldsymbol{x},\xi)\in\dot{T}^*(X) :\ \exists(\boldsymbol{s},t,(\eta',\eta_n))\in \mathrm{WF}_B(\mathbb{1}_A),\ \eta_n\neq 0,\ \boldsymbol{x}\in\mathcal{I}(\boldsymbol{s},t) :\ \mathrm{d}_{\boldsymbol{s}}\varphi(\boldsymbol{s},\boldsymbol{x}) = -\eta'/\eta_n,\ \xi = \eta_n\, \mathrm{d}_{\boldsymbol{x}}\varphi(\boldsymbol{s},\boldsymbol{x}))\big\}. \tag{42}$$

Note that $\mathrm{WF}_{\mathrm{supp}(Fu)}(\mathbb{1}_A) = \mathrm{WF}_B(\mathbb{1}_A)$, so we replace $\mathrm{supp}(Fu)$ by B in (42).

The proof of (42) will not be given because it is similar to the proof of (40) given in Proposition C.2, except, there is no $-\omega\, \mathrm{d}_{\boldsymbol{s}}\varphi(\boldsymbol{s},\boldsymbol{x}_0)$ term.

3.5. **Terminology for microlocal singularities and artifacts.** To better understand microlocal properties of Radon transforms and to motivate Definition 3.5 we now show that Radon transforms produce only singularities conormal to the manifolds of integration.

Proposition 3.4. *Let $(\boldsymbol{x},\xi)\in\dot{T}^*(X)$ and let A be a limited data set.*

(1) *Let $u\in\mathcal{E}'(X)$. If $(\boldsymbol{x},\xi)\in\mathrm{WF}(\mathcal{L}u)$, then for some $(\boldsymbol{s},t)\in A$, $(\boldsymbol{x},\xi)\in N^*(\mathcal{I}(\boldsymbol{s},t))$.*

(2) *If $(\boldsymbol{x},\xi)\notin N^*(\mathcal{I}(\boldsymbol{s},t))$ for any $(\boldsymbol{s},t)\in A$ then $(\boldsymbol{x},\xi)\notin\mathrm{WF}(\mathcal{L}u)$ for any $u\in\mathcal{E}'(X)$.*

Part (2) is the contrapositive of part (1), and it will be useful in the discussion of invisible singularities.

Proof of Proposition 3.4. We apply the Hörmander-Sato lemma, (11), to see that for any $u\in\mathcal{E}'(X)$,

$$\mathrm{WF}(\mathcal{L}u)\subset(\mathcal{C}_A)^\top\circ\mathrm{WF}(\mathbb{1}_A Fu)\subset\Pi_{\mathrm{L}}^{\mathcal{C}_A^\top}(\Pi_{\mathrm{R}}^{\mathcal{C}_A^\top})^{-1}(\dot{T}^*(Y)) = \Pi_{\mathrm{L}}^{\mathcal{C}_A^\top}(\mathcal{C}_A^\top), \tag{43}$$

where $\Pi_{\mathrm{L}}^{\mathcal{C}_A^\top}$ and $\Pi_{\mathrm{R}}^{\mathcal{C}_A^\top}$ are the natural projections from $\mathcal{C}_A^\top$ to $T^*(Y)$ and $T^*(X)$ respectively. We compose with $\mathcal{C}_A^\top$ because the only wave front directions of $\mathbb{1}_A F u$ are above A.

This containment shows that

$$\mathrm{WF}(\mathcal{L}u) \subset \Pi_{\mathrm{L}}^{\mathcal{C}_A^\top}(\mathcal{C}_A^\top) = \Pi_{\mathrm{R}}(\mathcal{C}_A),$$

and singularities in $\Pi_{\mathrm{R}}(\mathcal{C}_A)$ are of the form $(\boldsymbol{x}, \omega\, \mathrm{d}_{\boldsymbol{x}}\varphi(\boldsymbol{s}, \boldsymbol{x}_0))$ for some $(\boldsymbol{s}, t) \in A$, $\boldsymbol{x} \in \mathcal{I}(\boldsymbol{s}, t)$ and $\omega \in \dot{\mathbb{R}}$ since they are last coordinates in $\mathcal{C}_A$ (see (18)). Such singularities are exactly the conormal singularities to $\mathcal{I}(\boldsymbol{s}, t)$ since $\mathcal{I}(\boldsymbol{s}, t)$ is defined by $\varphi(\boldsymbol{s}, \boldsymbol{x}) = t$. Equivalently, such singularities are exactly those in the conormal bundle $N^*(\mathcal{I}(\boldsymbol{s}, t))$. This proves (1).

Part (2) is the contrapositive of part (1). □

This proposition motivates the following definition.

Definition 3.5. *Let $u \in \mathcal{E}'(X)$ and let $(\boldsymbol{x}, \xi) \in \dot{T}^*(X)$.*

(A) *First, assume $(\boldsymbol{x}, \xi) \in \mathrm{WF}(u)$.*
  (1) *If $(\boldsymbol{x}, \xi)$ is also in $\mathrm{WF}(\mathcal{L}u)$, then $(\boldsymbol{x}, \xi)$ is called a* (microlocal) visible singularity *of u (in $\mathcal{L}$).*
  (2) *If $(\boldsymbol{x}, \xi)$ is* not *in $\mathrm{WF}(\mathcal{L}u)$, then $(\boldsymbol{x}, \xi)$ is called an* (microlocal) invisible singularity *of u (in $\mathcal{L}$).*

(B) *Assume $(\boldsymbol{x}, \xi) \notin \mathrm{WF}(u)$. If $(\boldsymbol{x}, \xi) \in \mathrm{WF}(\mathcal{L}u)$, then $(\boldsymbol{x}, \xi)$ is called a* (microlocal) artifact.
  (1) *If $(\boldsymbol{x}, \xi) \in \mathrm{WF}(F^*Fu)$, it is called a* (microlocal) Bolker artifact[1].
  (2) *If $(\boldsymbol{x}, \xi) \in \mathrm{WF}(\mathcal{L}u)$ for some limited data set A but not in $\mathrm{WF}(F^*Fu)$, we call it a* (microlocal) limited data artifact.
    (i) *If a limited data artifact is in $\mathcal{C}_A^\top \circ \mathrm{WF}_{\mathrm{supp}(Fu)}(\mathbb{1}_A)$, it will be called an* object independent (limited data) artifact *because it does not depend on the microlocal properties of u, only $\mathrm{supp}(Fu)$.*
    (ii) *Otherwise, the artifact is an* object dependent (limited data) artifact *because it depends on whether Fu has singularities above $\mathrm{Bd}(A)$ or not.*

We call the artifacts in part (B) (1) Bolker artifacts because they can appear when F does not satisfy the Bolker condition (12), and so the normal operator for full data can create artifacts. If $F\colon \mathcal{E}'(X) \to \mathcal{D}'(Y)$ satisfies the Bolker condition, then there are no artifacts from backprojection of full data: if F^* and F can be composed, then for all $u \in \mathcal{E}'(X)$, $\mathrm{WF}(u) = \mathrm{WF}(F^*Fu)$, and if F^* and F cannot be composed, then $\mathrm{WF}(F^*\phi Fu) \subset \mathrm{WF}(u)$ for any smooth cutoff ϕ. We will discuss Bolker artifacts in Section 3.6.4.

We include "microlocal" in all of our terms to indicate these are non-smooth artifacts in the continuous problem. Smoothed versions of microlocal artifacts can appear as artifacts in a reconstruction with smoothing. They will not be microlocal singularities, but they can look like them.

By Proposition 3.4 part (1), the only singularities of u that could be visible in $\mathcal{L}u$ microlocally are conormal to some integration set $\mathcal{I}(\boldsymbol{s}, t)$ for some $(\boldsymbol{s}, t) \in A$. It should be pointed out that a singularity conormal to some $\mathcal{I}(\boldsymbol{s}, t)$ could be both a visible singularity and an artifact (for example, if the singularity is also conormal to $\mathcal{I}(\tilde{\boldsymbol{s}}, \tilde{t})$ for some $(\tilde{\boldsymbol{s}}, \tilde{t}) \in \mathrm{Bd}(A)$).

3.6. **An analysis of visible and invisible singularities and added artifacts in general.** All microlocal singularities and artifacts in $\mathcal{L}u$ are in at least one of the sets in (37). We now use this to describe how each of the sets in (37) can affect the reconstruction with $\mathcal{L}$. This will

[1] If F^* and F cannot be composed, then any artifact in $F^*\phi Fu$ for some smooth cutoff ϕ is a Bolker artifact.

characterize all types of microlocal artifacts and visible singularities in reconstruction from the operators of (22) and (23). Let $u \in L^1_c(X, \mathbb{R})$, and let A be a limited data set.

3.6.1. *Object dependent limited data artifacts.* The set

$$\left(\mathcal{C}^\top \circ M^{\mathrm{c}}(A,u)\right) \cup \left(\mathcal{C}^\top \circ M^{\mathrm{nc}}(A,u)\right)$$

represents possible object dependent artifacts since $M^{\mathrm{c}}(A,u)$ and $M^{\mathrm{nc}}(A,u)$ are generated by singularities of u above $\mathcal{I}(\boldsymbol{s},t)$ for $(\boldsymbol{s},t) \in B_2$.

As shown after (40), if $(\boldsymbol{s},t) \in B_2^{\mathrm{c}}$, then

$$\dot{N}^*(\mathcal{I}(\boldsymbol{s},t)) \subset \mathcal{C}_A^\top \circ M^{\mathrm{c}}(A,u), \tag{44}$$

and object dependent artifacts can be created all along $\mathcal{I}(\boldsymbol{s},t)$.

3.6.2. *Object independent limited data artifacts.* The set of object independent limited data artifacts are contained in $\mathcal{C}^\top \circ \mathrm{WF}_B(\mathbb{1}_A)$ since they depend only on A and $\mathrm{supp}(Fu)$, not the microlocal properties of u. The arc-shaped artifact in Figure 3 of Section 4 is an object independent artifact, as explained in that section.

3.6.3. *Visible singularities.* The set $\mathcal{C}_A^\top \circ M^{\mathrm{F}}(A,u)$ contains the visible singularities of u. This is true for the following reason: If $(\boldsymbol{x},\xi) \in \dot{T}^*(X)$ then a calculation using the composition (10) shows

$$(\boldsymbol{x},\xi) \in \mathcal{C}_A^\top \circ (\mathcal{C}_A \circ \{(\boldsymbol{x},\xi)\}),$$

so singularities of u that are in $\mathcal{L}u$ must be in this set. By Proposition 3.4, these are wave front directions $(\boldsymbol{x},\xi) \in \mathrm{WF}(u)$ such that there is a $(\boldsymbol{s},t) \in A$ such that $(\boldsymbol{x},\xi) \in \dot{N}^*(\mathcal{I}(\boldsymbol{s},t))$. The set $\mathcal{C}_A^\top \circ M^{\mathrm{F}}(A,u)$ might not contain all such conormal singularities of u, and it can contain artifacts which we now discuss.

3.6.4. *Bolker artifacts.* These artifacts can occur even with full data when $F\colon \mathcal{E}'(X) \to \mathcal{D}'(Y)$ does not satisfy the Bolker condition because F^*F can create artifacts. We will see such artifacts in Section 4.

Such artifacts are contained in $\mathcal{C}^\top \circ M^{\mathrm{F}}(A,u) \setminus \mathrm{WF}(u)$ (for full data, $\mathcal{C}^\top \circ M^{\mathrm{F}}(Y,u) \setminus \mathrm{WF}(u)$). They are object dependent artifacts since they depend on $\mathrm{WF}(u)$.

Putting this together with the discussion in Section 3.6.3 shows that $\mathcal{C}_A^\top \circ M^{\mathrm{F}}(A,u)$ contains both the visible singularities of u and the Bolker artifacts.

For limited data on A, Bolker artifacts can be created either when $\Pi_{\mathrm{L}}\colon \mathcal{C}_A \to T^*(Y)$ is not injective or when this map is not an immersion on $\mathcal{C}_A$.[2]

First, consider when $\Pi_{\mathrm{L}}\colon \mathcal{C}_A \to T^*(Y)$ is not injective. In this case, for some $(\boldsymbol{s},t,\eta) \in \dot{T}^*_A(Y)$ there are at least two points:

$$(\boldsymbol{s},t,\eta,\boldsymbol{x}_0,\xi_0) \text{ and } (\boldsymbol{s},t,\eta,\boldsymbol{x}_m,\xi_m) \text{ in } \mathcal{C}_A$$

that map to $(\boldsymbol{s},t,\eta)$ under Π_{L}. Since the $T^*(Y)$ coordinates are the same, we see

$$\boldsymbol{x}_0 \in \mathcal{I}(\boldsymbol{s},t),\ \boldsymbol{x}_m \in \mathcal{I}(\boldsymbol{s},t),\ \boldsymbol{x}_0 \neq \boldsymbol{x}_m, \text{ and } \mathrm{d}_{\boldsymbol{s}}\varphi(\boldsymbol{s},\boldsymbol{x}_0) = \mathrm{d}_{\boldsymbol{s}}\varphi(\boldsymbol{s},\boldsymbol{x}_m). \tag{45}$$

We can assert $\boldsymbol{x}_0 \neq \boldsymbol{x}_m$ because the ξ coordinate in $\mathcal{C}$ is determined by $(\boldsymbol{s},t,\eta,\boldsymbol{x})$, so if $\boldsymbol{x}_0 = \boldsymbol{x}_m$ for two preimages of $(\boldsymbol{s},t,\eta)$, then the ξ coordinates agree. After composing with $\mathcal{C}^\top$, one sees

$$\{(\boldsymbol{x}_0,\xi_0),(\boldsymbol{x}_m,\xi_m)\} \subset \mathcal{C}^\top \circ M^{\mathrm{F}}(A,u) = \mathcal{C}^\top \circ (\mathcal{C}_A \circ \mathrm{WF}(u)).$$

[2]That is, the derivative of $\Pi_{\mathrm{L}}\colon \mathcal{C}_A \to T^*(Y)$ is not injective at some point on $\mathcal{C}_A$.

So, if $(\boldsymbol{x}_0, \xi_0) \in \mathrm{WF}(u) \cap \Pi_{\mathrm{R}}(\mathcal{C}_A)$, then $(\boldsymbol{x}_0, \xi_0)$ and $(\boldsymbol{x}_m, \xi_m)$ can both be in $\mathrm{WF}(\mathcal{L}u)$, even if u does not have a singularity at $(\boldsymbol{x}_m, \xi_m)$. Such artifacts are often called *mirror point artifacts*. Note that if $(\boldsymbol{x}_0, \xi_0)$ does not create a singularity in Fu, then $(\boldsymbol{x}_0, \xi_0)$ will not be visible in $\mathcal{L}u$ and will not create any mirror point artifacts.

The curve of artifacts outside the unit disk in Figure 1 of the next section is made up of mirror point artifacts caused by the object in the unit disk.

The other type of Bolker artifact is when Π_{L} is not an immersion, but it is less common than the other artifacts. An example of a Bolker artifact caused when Π_{L} is not an immersion on all of $\mathcal{C}_A$ is in [39]. One can use the theory of $I^{p,l}$ classes of singular FIO to evaluate the strength of such artifacts [4, 18].

We now provide a summary of this analysis. Each microlocal singularity in $\mathrm{WF}(\mathcal{L}u)$ must be in at least one set in the containment (37), and each of the four sets in (37) can generate artifacts.

- Limited data artifacts are in $\mathcal{C}_A^\top \circ M^{\mathrm{c}}(A,u)$, $\mathcal{C}_A^\top \circ M^{\mathrm{nc}}(A,u)$, and $\mathcal{C}_A^\top \circ \mathrm{WF}_{\mathrm{supp}(Fu)}(\mathbb{1}_A)$, since such artifacts depend on $\mathrm{WF}_{\mathrm{supp}(Fu)}(\mathbb{1}_A)$.
- Object dependent limited data artifacts are in $\mathcal{C}_A^\top \circ M^{\mathrm{c}}(A,u)$, $\mathcal{C}_A^\top \circ M^{\mathrm{nc}}(A,u)$, since such artifacts depend on $\mathrm{WF}(\mathbb{1}_A)$ and $\mathrm{WF}(Fu)$.
- Object independent limited data artifacts are in $\mathcal{C}_A^\top \circ \mathrm{WF}_B(\mathbb{1}_A)$, since such artifacts do not depend on $\mathrm{WF}(Fu)$, only on $\mathrm{WF}(\mathbb{1}_A)$.
- Bolker artifacts are in $\mathcal{C}_A^\top \circ M^{\mathrm{F}}(A,u)$ because they do not depend on singularities of $\mathbb{1}_A$ but on whether F satisfies the Bolker condition. If the Bolker condition holds, then there are no Bolker artifacts. If it does not hold, then there can be Bolker artifacts in $\mathcal{C}_A^\top \circ M^{\mathrm{F}}(A,u)$.
- There can be both object independent and object dependent artifacts caused by singularities of $\mathbb{1}_A Fu$ above the same base point in B_2 (see Figure 3 and Remark C.5).
- Finally, these sets contain all microlocal artifacts and visible singularities in $\mathcal{L}u$ because $\mathrm{WF}(\mathcal{L}u)$ is contained in the union of these sets by (37).

We now use our methodology with two common assumptions about F and $\mathcal{C}$ to better understand the sets in (38)-(40).

3.7. **Case I: The best case.** We now assume F and its canonical relation $\mathcal{C}$ satisfies the following properties.

(I.1) The Bolker condition holds for $F\colon \mathcal{E}'(X) \to \mathcal{D}'(Y)$, i.e. $\Pi_{\mathrm{L}}\colon \mathcal{C} \to T^*(Y)$ is an injective immersion.

(I.2) The projection $\Pi_{\mathrm{R}}\colon \mathcal{C} \to \dot{T}^*(X)$ is injective. This means that for each $(\boldsymbol{x}, \xi) \in \dot{T}^*(X)$ there is at most one $(\boldsymbol{s}, t) \in Y$ such $(\boldsymbol{x}, \xi) \in N^*(\mathcal{I}(\boldsymbol{s}, t))$.

Therefore, there are no Bolker artifacts for transforms satisfying (I.1) and (I.2).

We point out that (I.1) and (I.2) imply that $\Pi_{\mathrm{R}}\colon \mathcal{C} \to T^*(X)$ is also an injective immersion where injectivity follows from (I.2) and immersion follows from [23, Propositions 4.1.3 and 4.1.4]. Since $\Pi_{\mathrm{R}}\colon \mathcal{C} \to T^*(X)$ is equivalent to $\Pi_{\mathrm{L}}^{\mathcal{C}^\top}\colon \mathcal{C}^\top \to T^*(X)$ by switching coordinates, F^* also satisfies the Bolker condition.

The assumptions of Case I hold for the Radon hyperplane transform in $\mathbb{R}^n$.[3] An analysis of the artifacts and visible singularities for limited angle tomography is in [11, 26, 34], and

[3]This is true when the transform is parameterized by hyperplanes or $\left(S^{n-1} \times \mathbb{R}\right) / \sim$ where $S^{n-1} \times \mathbb{R} \ni (\omega, p) \sim (-\omega, -p)$. The weight $H(\boldsymbol{x}, \omega)$ must be even in ω.

a generalization to the hyperplane transform in $\mathbb{R}^n$ is given in [13]. A complete analysis for arbitrary limited X-ray CT data in the plane is done in [7].

We will study the region of interest problem for this transform in the plane–the X-ray transform–in Section 4.2.

The assumptions of this section also hold for the common offset seismic transform with constant sound velocity for objects below the ocean surface [9, 31]. This transform will be discussed in depth in Section 4.3.1.

Theorem 3.6 (Visible and invisible singularities)**.** *Let X be an open subset of $\mathbb{R}^n$ and $Y = \mathtt{S}\times\mathbb{R}$ for some open $\mathtt{S} \subset \mathbb{R}^{n-1}$. Assume (I.1) and (I.2) hold.*

Let A be a limited data set and let $\mathcal{L}$ be the limited data reconstruction operator given in (22). Finally, let $u \in L^1_c(X,\mathbb{R})$.

Let $(\boldsymbol{x},\xi) \in \Pi_{\mathrm{R}}(\mathcal{C})$. Let $(\boldsymbol{s},t)$ be the unique point in Y such that $(\boldsymbol{x},\xi) \in \dot{N}^*(\mathcal{I}(\boldsymbol{s},t))$.

(a) *If $(\boldsymbol{s},t) \in \mathrm{Int}(A)$, then*

$$(\boldsymbol{x},\xi) \in \mathrm{WF}(u) \text{ if and only if } (\boldsymbol{x},\xi) \in \mathrm{WF}(\mathcal{L}u).$$

(b) *If $(\boldsymbol{s},t) \in \mathrm{Ext}(A)$, then $(\boldsymbol{x},\xi) \notin \mathrm{WF}(\mathcal{L}u)$. In this case, any singularity of u at $(\boldsymbol{x},\xi)$ will be an invisible singularity of u in $\mathcal{L}u$.*

Proof. To prove (a), let $(\boldsymbol{s},t) \in \mathrm{Int}(A)$ and $(\boldsymbol{x}, \omega\, \mathrm{d}_{\boldsymbol{x}}\varphi(\boldsymbol{s},\boldsymbol{x}))$ be an arbitrary point in

$$\dot{N}^*(\mathcal{I}(\boldsymbol{s},t)) \cap \mathrm{WF}(u).$$

As noted at the start of this section, F^* satisfies the Bolker condition. We prove part (a) using the following equivalences:

$(\boldsymbol{x}, \omega\, \mathrm{d}_{\boldsymbol{x}}\varphi(\boldsymbol{s},\boldsymbol{x})) \in \mathrm{WF}(u) \cap \dot{N}^*(\mathcal{I}(\boldsymbol{s},t))$
if and only if $(\boldsymbol{s},t,(-\omega\, \mathrm{d}_{\boldsymbol{s}}\varphi(\boldsymbol{s},\boldsymbol{x}),\omega)) \in \mathrm{WF}(Fu)$ (by Bolker and (18))
if and only if $(\boldsymbol{s},t,(-\omega\, \mathrm{d}_{\boldsymbol{s}}\varphi(\boldsymbol{s},\boldsymbol{x}),\omega)) \in \mathrm{WF}(\mathbb{1}_A Fu)$ (as $(\boldsymbol{s},t) \in \mathrm{Int}(A)$)
if and only if $(\boldsymbol{x}, \omega\, \mathrm{d}_{\boldsymbol{x}}\varphi(\boldsymbol{s},\boldsymbol{x})) \in \mathrm{WF}(\mathcal{L}u)$ (as F^* satisfies Bolker and F^* can be composed with $\mathbb{1}_A F$ without a cutoff).

The proof for part (b) is similar to the proof of (a) but it uses that $(\boldsymbol{s},t) \in \mathrm{Ext}(A)$, so $\mathbb{1}_A Fu$ is zero near $(\boldsymbol{s},t)$, and finally that F^* satisfies the Bolker condition. □

Remark 3.7. *If the only covectors in $\mathrm{WF}_B(\mathbb{1}_A)$ have second coordinate of the form $(\eta',0)$ then $\mathcal{C}^\top \circ \mathrm{WF}_B(\mathbb{1}_A) = \emptyset$. This is true because every covector in $\mathcal{C}$ has a nonzero $\mathrm{d}t$ coordinate as can be seen from (18). Therefore, $M^{\mathrm{c}}(A,u) = \emptyset$. In this case, there are no object independent artifacts.*

Limited angle X-ray CT is a good example of this as shown in [11].

Theorem 3.8 (Added Artifacts)**.** *Let X be an open subset of $\mathbb{R}^n$ and $Y = \mathtt{S}\times\mathbb{R}$ for some open $\mathtt{S} \in \mathbb{R}^{n-1}$. Assume (I.1) and (I.2). Let A be a limited data set and let $\mathcal{L}$ be the limited data reconstruction operator given in (22). Let $u \in L^1_c(X,\mathbb{R})$*

Let $(\boldsymbol{s},t) \in \mathrm{Bd}(A)$ and assume Fu is smooth[4] and nonzero near $(\boldsymbol{s},t)$. If $\lambda = (\boldsymbol{s},t,\eta) \in \mathrm{WF}(\mathbb{1}_A) \cap \Pi_{\mathrm{L}}(\mathcal{C}_A)$, then $\mathcal{C}^\top \circ \{\lambda\} \in \mathrm{WF}(\mathcal{L}u)$.

This theorem shows that object independent artifacts *will* be created when Fu is smooth and nonzero near $(\boldsymbol{s},t) \in \mathrm{Bd}(A)$.

Proof. Since Fu is smooth and nonzero near $(\boldsymbol{s},t)$, the singularities of $\mathbb{1}_A Fu$ above $(\boldsymbol{s},t)$ are the same as those of $\mathbb{1}_A$, so $\lambda \in \mathrm{WF}(\mathbb{1}_A Fu) \cap \Pi_{\mathrm{L}}(\mathcal{C}_A)$. Since F^* satisfies the Bolker condition and is elliptic, this is mapped to a singularity of $\mathcal{L}u$ as indicated in the theorem. □

[4]This condition is true if $\mathrm{WF}(u) \cap N^*(\mathcal{I}(\boldsymbol{s},t)) = \emptyset$.

Using (37), we can divide the singularities generated by $\mathcal{L}$ as follows.

$$\begin{aligned}
&\mathrm{WF}(\mathcal{L}u) \subset \mathcal{A}(A,u) \cup \mathcal{V}(A,u) \text{ where}\\
&\mathcal{A}(A,u) = \left(\mathcal{C}_A^\top \circ M^{\mathrm{c}}(A,u)\right) \cup \left(\mathcal{C}_A^\top \circ M^{\mathrm{nc}}(A,u)\right) \cup \left(\mathcal{C}_A^\top \circ \mathrm{WF}_B(\mathbb{1}_A)\right),\\
&\mathcal{V}(A,u) = \mathcal{C}_A^\top \circ M^{\mathrm{F}}(A,u).
\end{aligned}$$

By the Bolker condition, the set $\mathcal{V}(\mathrm{Int}(A),u)$ contains all possible visible singularities of u that are in some $\dot{N}^*(\mathcal{I}(\boldsymbol{s},t))$ for $(\boldsymbol{s},t) \in \mathrm{Int}(A)$. The set $\mathcal{A}(A,u)$ contains the limited data artifacts.

3.8. **Case II.** In this section, we will examine the artifacts that occur in a more general case that is illustrated by the PAT transform in Example 3.10 and in Section 4.1.

Let X be an open subset of $\mathbb{R}^n$ and let Ω be an open subset of X. Let $\mathtt{S}$ be an open subset of $\mathbb{R}^{n-1}$ and let $Y = \mathtt{S}\times\mathbb{R}$. Let $F\colon \mathcal{E}'(X) \to \mathcal{D}'(Y)$ be a Radon transform and let $\mathcal{C} \subset T^*(Y\times X)$ be the canonical relation of F. Let

$$\mathcal{C}_\Omega = \{(\boldsymbol{s},t,\eta,\boldsymbol{x},\xi) \in \mathcal{C} :\ \boldsymbol{x} \in \Omega\}.$$

For Case II, we have the following assumptions.

(II.1) We assume $\Pi_{\mathrm{L}}\colon \mathcal{C}_\Omega \to T^*(Y)$ satisfies the Bolker condition, (12).

(II.2) We assume for each $(\boldsymbol{s},t,\eta) \in \Pi_{\mathrm{L}}(\mathcal{C}_\Omega)$ there are $k>1$ number of preimages of $(\boldsymbol{s},t,\eta)$ in the full canonical relation $\mathcal{C}$. That is for each $(\boldsymbol{s},t,\eta) \in \Pi_{\mathrm{L}}(\mathcal{C}_\Omega)$ there are $k>1$ covectors $(\boldsymbol{x}_j,\xi_j) \in T^*(X)$ such that $(\boldsymbol{s},t,\eta;\boldsymbol{x}_j,\xi_j) \in \mathcal{C}$ for $j=1,\dots,k$, where k depends on $(\boldsymbol{s},t,\eta)$.

Theorem 3.9. *Assume $F\colon \mathcal{E}'(X) \to \mathcal{D}'(Y)$ satisfies (II.1) and (II.2). Let $u \in \mathcal{E}'(X)$.*

Then, for each $(\boldsymbol{s},t,\eta) \in \Pi_{\mathrm{L}}(\mathcal{C}_\Omega)$, only one of the $\boldsymbol{x}_j$ in (II.2) is in Ω.

For each singularity $(\boldsymbol{x},\xi) \in \Pi_{\mathrm{R}}(\mathcal{C}_\Omega) \cap \mathrm{WF}(u)$, there can be mirror point artifacts for F^*Fu outside of Ω, each one corresponding to a $(\boldsymbol{s},t,\eta)$ such that $(\boldsymbol{x},\xi) \in \dot{N}^*\mathcal{I}(\boldsymbol{s},t)$.

For each $(\boldsymbol{s},t,\eta) \in \Pi_{\mathrm{L}}(\mathcal{C}_\Omega)$ we will assume, without loss of generality, that $\boldsymbol{x}_1 \in \Omega$.

Proof. Because $\Pi_{\mathrm{L}}\colon \mathcal{C}_\Omega \to T^*(Y)$ is injective, for each $(\boldsymbol{s},t,\eta) \in \Pi_{\mathrm{L}}(\mathcal{C}_\Omega)$ only one of the $\boldsymbol{x}_j$ is in Ω.

We now calculate $\mathcal{C}^\top \circ (\mathcal{C}_\Omega \circ \{(\boldsymbol{x}_1,\eta_1)\})$. We can compose with $\mathcal{C}_\Omega$ since u is supported in Ω.

Let $(\boldsymbol{x}_1,\xi_1) \in \Pi_{\mathrm{R}}(\mathcal{C}_\Omega) \cap \mathrm{WF}(u)$ and let $(\boldsymbol{s},t,\eta) \in \dot{T}^*(Y)$ such that

$$\lambda_1 = (\boldsymbol{s},t,\eta,\boldsymbol{x}_1,\xi_1) \in \mathcal{C}_\Omega.$$

Note that $(\boldsymbol{x}_1,\xi_1) \in N^*(\mathcal{I}(\boldsymbol{s},t))$ by the proof of Proposition 3.4.

Then,

$$(\boldsymbol{s},t,\eta) \in \mathcal{C} \circ \{(\boldsymbol{x}_1,\xi_1)\}$$

since $\lambda_1 \in \mathcal{C}$ and by assumption, there are covectors $(\boldsymbol{x}_j,\xi_j) \in T^*(X)$ for $j=2,k$ such that $(\boldsymbol{x}_j,\eta_j,\boldsymbol{s},t,\eta) \in \mathcal{C}^\top$ and $\boldsymbol{x}_j \notin \Omega$. Therefore, each covector in $\mathcal{C} \circ \{(\boldsymbol{x}_1,\xi_1)\}$ generates a finite number of possible artifacts with base points outside of Ω.

If Ω is pre-compact, one can show there are only a finite number of artifact points for each $(\boldsymbol{x}_1,\xi_1)$ because there are only a finite number of preimages of $(\boldsymbol{x}_1,\xi_1)$ under Π_{R} by [15, Lemma 3.1]. □

Example 3.10. *Let Ω be the open unit disk in $\mathbb{R}^2$. The circular transform discussed in Section 4.1 satisfies the Bolker assumption above Ω, i.e., $\Pi_{\mathrm{L}}\colon \mathcal{C}_\Omega \to T^*(Y)$ is an injective immersion, and the reconstruction operator $F^*F\colon \mathcal{E}'(\Omega) \to \mathcal{D}'(\Omega)$ is an elliptic ΨDO, as noted there.*

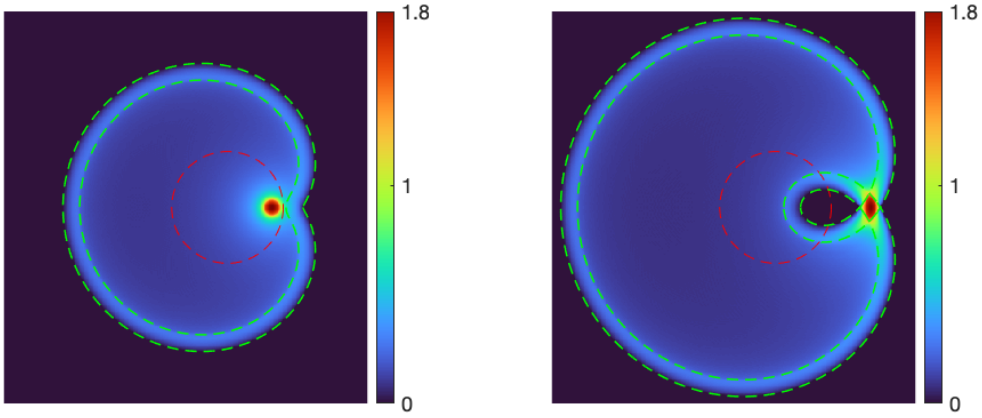

FIGURE 1. Numerical approximations of $F^*Fu|_{[-4,2.5]\times[-3.5,3.5]}$ for the indicator functions $u = \mathbb{1}_{B_{0.15}(0.8,0)}$ (left) and $u = \mathbb{1}_{B_{0.15}(1.7,0)}$ (right) where F is the spherical Radon transform with centers on the boundary of the unit disk Ω, see Section 4.1. The dashed red curve indicates $\mathrm{Bd}(\Omega)$, and the dashed green curves are the predicted artifact curves γ_- and γ_+, see (48) for the situation on the left. These curves are not part of F^*Fu.

This transform does not satisfy the conditions in Case I. *Let* $(\boldsymbol{x},\xi) \in \dot{T}^*(\Omega)$. *Then, the line through* $\boldsymbol{x}$ *and in direction* ξ *intersects* S^1 *in two points* $\mathbf{c}_1$ *and* $\mathbf{c}_2$. *The covector* $(\boldsymbol{x},\xi)$ *is conormal to the two circles centered at* $\mathbf{c}_j$ *of radius* $|\boldsymbol{x}-\mathbf{c}_j|$, $j=1,2$. *Therefore, (I.2) fails for this transform.*

However, the transform satisfies the conditions in Case II. *As shown in that section, if* $(\boldsymbol{x},\xi) \in \dot{T}^*(\Omega)$, *then there are mirror point artifacts outside of* Ω *if one reconstructs objects inside* Ω *at points outside* Ω.

The PAT transform also has covectors, $\lambda \in \mathcal{C}$ *at which* Π_{L} *is not an immersion* [2]. *However,* $\Pi_{\mathrm{R}}(\lambda)$ *has base point outside of* Ω, *and such covectors,* λ, *do not affect reconstructions in* Ω *for* $u \in \mathcal{E}'(\Omega)$.

3.9. **Case III: When Π_{L} is not an immersion.** As noted in Section 3.6.4, this case is more difficult, and different types of artifacts exist as in [3, 10, 18, 39]. We will not consider this case.

4. ARTIFACT ANALYSIS FOR THE LIMITED DATA OPERATOR IN 2D

In this section, we demonstrate the versatility of our artifact analysis through a variety of 2D examples.

4.1. **The spherical Radon transform.** The spherical Radon transform (spherical mean operator) with sources and receivers at the same positions on a sphere is a model for photoacoustic or thermoacoustic tomography, see, e.g., [27]. Mirror artifacts can occur with this transform.

We consider the problem in $\mathbb{R}^2$ and the center set is S^1, the unit circle. Define $\varphi\colon \mathbb{R}\times\mathbb{R}^2 \to [0,\infty)$ by $\varphi(s,\boldsymbol{x}) = |\boldsymbol{x}-\Theta(s)|$ where $\Theta(s) = (\cos s, \sin s)^\top \in S^1$. Then, $F\colon \mathcal{E}'(\mathbb{R}^2\setminus S^1) \to \mathcal{D}'(\mathbb{R}\times(0,\infty))$, $Fu(s,t) = \int_{\mathbb{R}^2} u(\boldsymbol{x})\,\delta(t-\varphi(s,\boldsymbol{x}))\mathrm{d}\boldsymbol{x}$, integrates u along the circle of radius t with $\Theta(s)$ as its center. Note that F is an FIO from $\mathcal{E}'(\mathbb{R}^2\setminus S^1)$ to $\mathcal{D}'(\mathbb{R}\times(0,\infty))$ and $Fu(s,t)$ is $2\pi-$periodic in s because Θ is.

The dual operator F^* is defined for continuous functions g on $\mathbb{R}\times(0,\infty)$ by

$$F^*g(\boldsymbol{x}) = \int_0^{2\pi} g(s,|\boldsymbol{x}-\Theta(s)|)\,\mathrm{d}s, \tag{46}$$

and, although the integral for F^* is over $[0,2\pi]$, F^* can be written as a FIO on domain $\mathcal{D}'(\mathbb{R}\times(0,\infty))$ using cutoffs in a way that is independent of the cutoffs for $2\pi-$periodic distributions, see Remark 4.1 below. For the microlocal properties of F and F^* we refer to [2].

Remark 4.1. *We now construct the FIO F^*. Let ϕ_1 and ϕ_2 be a partition of unity on S^1 subordinate to the coordinate patches $\Theta((-\pi,\pi))$ and $\Theta((0,2\pi))$, and let $\varphi_1=\phi_1\circ\Theta$ and $\varphi_2=\phi_2\circ\Theta$ be their pullbacks to smooth $2\pi-$periodic functions on $\mathbb{R}$. Note that $\varphi_1+\varphi_2=1$. Let $g(s,t)$ be a continuous function that is $2\pi-$periodic in s, and let F_1^* be defined as in (46) but integrating over $[-\pi,\pi]$. By periodicity, $F_1^*g=F^*g$. Therefore, when g is $2\pi-$periodic, $F^*g=F^*(\varphi_1 g+\varphi_2 g)=F_1^*(\varphi_1 g)+F^*(\varphi_2 g)$ independent of the choice of ϕ_1 and ϕ_2.*

Note that $g\mapsto F_1^*(\varphi_1 g)+F^*(\varphi_2 g)$ is an FIO for $g\in\mathcal{D}'(\mathbb{R}\times(0,\infty))$ because the integral for $F^*(\varphi_2 g)$ is with respect to $\varphi_2(s)\,\mathrm{d}s$ not $\mathbb{1}_{[0,2\pi]}(s)\mathrm{d}s$ and similarly for $g\mapsto F_1^*(\varphi_1 g)$. This shows that we can define $F^*\colon\mathcal{D}'(\mathbb{R}\times(0,\infty))\to\mathcal{D}'(\mathbb{R}^2\backslash S^1)$ to be an FIO, and for periodic distributions, the definition is independent of ϕ_1 and ϕ_2.

The Bolker condition, see Definition 2.10, fails for F on $\mathbb{R}^2$ because Π_{L} is not injective. We will show that mirror artifacts may emerge from visible singularities of u according to (38) and (45). Let $s\in\mathbb{R}$ and let $\boldsymbol{x}_0\in\mathbb{R}^2\backslash S^1$. Let C be the circle centered at $\Theta(s)$ and containing $\boldsymbol{x}_0$. Now assume $(\boldsymbol{x}_0,\xi)\in N^*(C)\cap\mathrm{WF}(u)$. By (45) and a calculation of $\partial_s\varphi$, a mirror point artifact in F^*Fu can occur at $\boldsymbol{x}_1\in C$ if

$$(\boldsymbol{x}_0-\Theta(s))\cdot\Theta(s)^\perp=(\boldsymbol{x}_1-\Theta(s))\cdot\Theta(s)^\perp, \tag{47}$$

where $\Theta(s)^\perp=\Theta(s+\pi/2)$. This shows that $\boldsymbol{x}_1$ is the reflection of $\boldsymbol{x}_0$ in the tangent line to S^1 at $\Theta(s)$ and therefore is the mirror point artifact to $\boldsymbol{x}_0$ (note that $\boldsymbol{x}_1\notin\mathrm{Cl}(\Omega)$). As a consequence, Π_{L} is not injective on $\mathbb{R}^2$.

For $\boldsymbol{x}\in\mathbb{R}^2$ and $r>0$ let $B_r(\boldsymbol{x})$ be the open ball centered at $\boldsymbol{x}$ of radius r. Let $\Omega=B_1(\mathbf{0})$ be the open unit ball.

For instance, $u=\mathbb{1}_{B_r(\boldsymbol{x}_c)}$, $\boldsymbol{x}_c\in\Omega$, $0<r<1-|\boldsymbol{x}_c|$, may create the concentric curves

$$\gamma_\pm(s)=(1+2c_\pm(s))\Theta(s)+\frac{\ell(s)\pm r}{\ell(s)}(\boldsymbol{x}_c-\Theta(s)) \tag{48}$$

with

$$\ell(s)=|\boldsymbol{x}_c-\Theta(s)|\quad\text{and}\quad c_\pm(s)=(\ell(s)\pm r)\sin\left(\arccos\left(\frac{\Theta(s)^\perp\cdot\boldsymbol{x}_c}{\ell(s)}\right)\right)$$

as artifact curves in F^*Fu. The left image of Figure 1 displays a numerical approximation to $F^*F\mathbb{1}_{B_{0.15}(0.8,0)}$. The predicted artifacts outside of Ω are clearly visible. Inside Ω no artifacts will emerge because the Bolker condition holds in Ω. The right image of Figure 1 shows $F^*F\mathbb{1}_{B_{0.15}(1.7,0)}$. The situation is different since not all wave fronts of $\mathbb{1}_{B_{0.15}(1.7,0)}$ are visible. In fact, for points near to the north and south pole of $\mathrm{Bd}(B_{0.15}(1.7,0))$ there are no spheres centered on $\mathrm{Bd}(\Omega)$ that are tangent to $\mathrm{Bd}(B_{0.15}(1.7,0))$ at these points. Nevertheless, analytical formulas for artifact curves $\gamma_\pm$ similar to (48) have been derived by us, but are more involved.[5]

While $\mathbb{1}_{B_{0.15}(0.8,0)}$ is clearly recognizable as a bright circular spot in its reconstructed image, the image of $\mathbb{1}_{B_{0.15}(1.7,0)}$ is an ellipse elongated in the north/south direction with blurred

[5]For these formulas see the MATLAB code under https://bwsyncandshare.kit.edu/s/QD8ASS5WzzMCre7 which has been used for creating the images displayed in Figure 1.

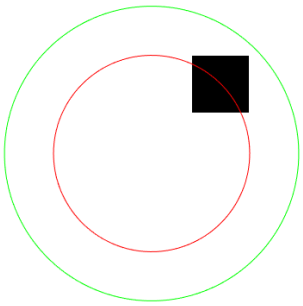

FIGURE 2. Illustration of u from (50) where white and black represent the numerical values 0 and 1, respectively. The circles indicate the boundaries of Ω (green) and the ROI $B_{2/3}(\mathbf{0})$ (red).

boundaries around the north and south poles. These are the invisible singularities as explained above.

4.2. **Region-of-interest tomography.** Here we consider the interior problem or region-of-interest (ROI) tomography for the classical Radon transform in 2D, see [22, 32, 33] for analytical and numerical results. The artifacts that occur have been analyzed before in [7, Section 4.3].

Let $\Omega = B_1(\mathbf{0})$ and define $\varphi\colon \mathbb{R}\times\Omega \to (-1,1)$ by $\varphi(s,\boldsymbol{x}) = \boldsymbol{x}^\top\Theta(s)$ where $\Theta(s)$ is the unit vector as defined in Section 4.1. Then, $F\colon L^2(\Omega) \to L^2([0,\pi]\times(-1,1))$, $Fu(s,t) = \int_\Omega u(\boldsymbol{x})\,\delta(t-\varphi(s,\boldsymbol{x}))\mathrm{d}\boldsymbol{x}$, integrates n along the straight line $\mathcal{I}(s,t)$ which is perpendicular to $\Theta(s)$ and having the signed distance t to the origin (parallel scanning geometry). For this setting, a filtered backprojection-type inversion formula is known:

$$u = \frac{1}{2\pi}F^*(\mathrm{Id}\otimes H\partial)Fu, \quad u\in L^2(\Omega), \tag{49}$$

where F^* is the classical backprojection operator (formal L^2 adjoint), H is the Hilbert transform, and ∂ denotes the first order differential operator, see, e.g., [40, eqn. (3.10)].

Remark 4.2. *Note that F is an FIO from $\mathcal{E}'(\Omega)$ to $\mathcal{D}'(\mathbb{R}\times(-1,1))$ and F maps into distributions that are $2\pi-$periodic in Θ. Using similar arguments to those in Remark 4.1, one can show F^* is an FIO that is consistently defined for $2\pi-$periodic distributions in s (for such distributions, F^* will integrate over $[0,2\pi]$, and then the factor in the reconstruction formula (49) becomes $\frac{1}{4\pi}$).*

We speak of an interior problem when the lateral variable t of the Radon data Fn is limited to $[-t_0,t_0]$ for $0<t_0<1$. Then n is no longer uniquely determined, even in the ROI $\mathrm{Cl}(B_{t_0}(\mathbf{0}))$, see [22]. So, ROI-tomography is modeled by the operator

$$\mathrm{Id}_{t_0} = \frac{1}{2\pi}F^*(\mathrm{Id}\otimes H\partial)\mathbb{1}_{A(t_0)}F, \quad A(t_0) = [0,\pi]\times[-t_0,t_0].$$

Now we investigate the types of artifacts that might appear in $\mathrm{Id}_{t_0}n$ according to the inclusion (37) which also holds for Id_{t_0} since $\mathrm{Id}\otimes H\partial$ is an elliptic ΨDO (see the discussion about compositions with special singular ΨDO starting around equation (22) in [15, Proof of Theorem 3.2]). To this end, let

$$t_0 = 2/3,\ \ A = A(2/3),\ \ u = \mathbb{1}_{I^2} \quad \text{for } I = \left[2\nu/3, 2/3\right] \text{ with } \nu = \sqrt{2}-1, \tag{50}$$

see Figure 2 for the underlying geometric setting.

First, we consider the set $\mathrm{WF}(\mathbb{1}_A)$ in (36). We emphasize that we have effectively no restriction on the angular variable s. Because of periodicity and symmetry, we could have chosen $A = \mathbb{R}\times[-2/3, 2/3]$, see Remark 4.2. So, the only singularities of $\mathbb{1}_A$ are those of $\mathbb{1}_{\mathbb{R}\times[-2/3,2/3]}$, yielding

$$\mathrm{WF}(\mathbb{1}_A) = \big\{\big((s, \pm 2/3), (0, \omega)\big) : s \in [0, \pi],\, \omega \in \dot{\mathbb{R}}\big\}.$$

Due to (29) and $\partial_s\varphi(s, \boldsymbol{x}) = \boldsymbol{x}^\top\Theta(s)^\perp = -x_1\sin(s) + x_2\cos(s)$ we have that

$$\begin{aligned}\mathrm{WF}(Fu) \subset\\ \big\{\big((0, 2\nu/3), \omega(-x_2, 1)\big) : x_2 \in I,\, \omega \in \dot{\mathbb{R}}\big\} \cup \big\{\big((0, 2/3), \omega(-x_2, 1)\big) : x_2 \in I,\, \omega \in \dot{\mathbb{R}}\big\}\\ \cup \big\{\big((\pi/2, 2\nu/3), \omega(x_1, 1)\big) : x_1 \in I,\, \omega \in \dot{\mathbb{R}}\big\} \cup \big\{\big((\pi/2, 2/3), \omega(x_1, 1)\big) : x_1 \in I,\, \omega \in \dot{\mathbb{R}}\big\}\\ \cup \big\{\big((s, \varphi(s, \boldsymbol{c})), \omega(-\boldsymbol{c}^\top\Theta(s)^\perp, 1)\big) : s \in [0, \pi],\, \omega \in \dot{\mathbb{R}},\, \boldsymbol{c} \text{ is a corner of } I^2\big\}.\end{aligned}$$

The first four sets are singularities of Fu generated by singularities of u above the sides of I^2 and the last set contains singularities of Fu generated by singularities of u at the corners $\boldsymbol{c}$ of I^2. Since F satisfies the Bolker condition, these really are singularities of Fu.

So, the only base points above which both $\mathbb{1}_A$ and Fu have singularities are $(0, 2/3)$ and $(\pi/2, 2/3)$. We have

$$\mathrm{WF}_{(0,2/3)}(\mathbb{1}_A) = \{\omega(0, 1) : \omega \in \dot{\mathbb{R}}\} \quad \text{and} \quad \mathrm{WF}_{(0,2/3)}(Fu) = \{\rho(-x_2, 1) : x_2 \in I,\ \rho \in \dot{\mathbb{R}}\}$$

as well as

$$\mathrm{WF}_{(\pi/2,2/3)}(\mathbb{1}_A) = \{\omega(0, 1) : \omega \in \dot{\mathbb{R}}\} \quad \text{and} \quad \mathrm{WF}_{(\pi/2,2/3)}(Fu) = \{\rho(x_1, 1) : x_1 \in I,\, \rho \in \dot{\mathbb{R}}\}.$$

Thus, the non-cancellation condition holds at both $(0, 2/3)$ and $(\pi/2, 2/3)$. This shows that $M^{\mathrm{c}}(A, u) = \emptyset$.

Continuing the calculation, we see that

$$\begin{aligned}\mathcal{C}^\top \circ M^{\mathrm{nc}}(A, u) = \big\{(2/3, y, \xi_1, 0) :\ y \in \dot{\mathbb{R}},\, \xi_1 \in \dot{\mathbb{R}}\big\}\\ \cup \big\{(x, 2/3, 0, \xi_2) :\ x \in \dot{\mathbb{R}},\, \xi_2 \in \dot{\mathbb{R}}\big\}.\end{aligned} \tag{51}$$

The base points form straight lines which contain the right and upper boundary of I^2, respectively, see Figure 3 (left).[6] We only validate that the set on the right belongs to $\mathcal{C}^\top \circ M^{\mathrm{nc}}(A, u)$ using (41). The other set can be handled in a similar way. Let $\eta = \omega(0, 1) \in \mathrm{WF}_{(\pi/2,2/3)}(\mathbb{1}_A)$, that is, $\omega \neq 0$, and $\nu = \rho(x_1, 1) \in \mathrm{WF}_{(\pi/2,2/3)}(Fu)$, that is, $\rho \neq 0$ and $x_1 \in I$. Then, $\eta' = 0$ and $\nu' = \rho x_1$. So we have

$$\begin{aligned}\mathcal{C}^\top \circ M^{\mathrm{nc}}(A, u) = \big\{\big(\boldsymbol{x}, (\omega + \rho)(0, 1)\big) :\ \omega + \rho \neq 0,\ \boldsymbol{x} \in \mathcal{I}(\pi/2, 2/3),\\ \exists \boldsymbol{y} \in \mathcal{X}(\pi/2, 2/3, u) : \partial_s\varphi(\pi/2, \boldsymbol{x}) = -\rho\, y_1/(\omega + \rho)\big\}.\end{aligned} \tag{52}$$

Here, $\mathcal{X}(\pi/2, 2/3, u) = I \times \{2/3\}$, which is the upper edge of I^2. Since $\partial_s\varphi(\pi/2, \boldsymbol{x}) = -x_1$,

$$x_1 = \frac{\rho}{\omega + \rho}\, y_1, \quad y_1 \in I.$$

Therefore, for each $y_1 \in I$, x_1 can be any number in $\mathbb{R}$ except 0 (since $\rho \neq 0$) and y_1 (since $\omega \neq 0$), and singularities from $M^{\mathrm{nc}}(A, u)$ above $(\pi/2, 2/3)$ generate artifacts above $(x_1, 2/3)$ for all $x_1 \notin \{0, y_1\}$. However, by choosing another point $\boldsymbol{y}' \in (I \setminus \{y_1\}) \times \{2/3\}$, one can generate a singularity at $(y_1, 2/3, 0, 1)$ in the same way.

[6] The MATLAB code which produces both images of Figure 3 can be downloaded from https://bwsyncandshare.kit.edu/s/fj3mPpocRqJ93ws.

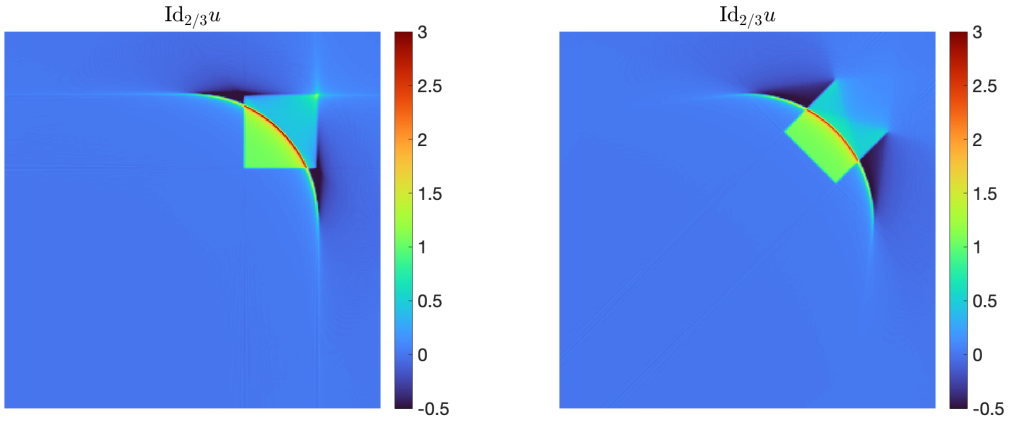

FIGURE 3. Numerical approximation of $\mathrm{Id}_{2/3}u$ for $u = \mathbb{1}_{I^2}$ (50) (left) and $u = \mathbb{1}_{QI^2}$ (right) where Q is the rotation by $\pi/4$ around the center of I^2. The underlying geometric constellation for the setting of the left image is depicted in Figure 2.

As shown above, the covectors $(0, 2/3, 0, \rho)$ and $(2/3, 0, \rho, 0)$ for $\rho \in \dot{\mathbb{R}}$ are not in $M^{\mathrm{nc}}(A, u)$, but both covectors are in $\mathcal{C}^\top \circ \mathrm{WF}(\mathbb{1}_A)$ by a calculation we will discuss below. Therefore, these $(0, 2/3, 0, \rho)$ is an object independent artifact, and artifacts are all along the lines $\mathcal{I}(0, 2/3)$ and $\mathcal{I}(\pi/2, 2/3)$.

For convenience, we let $\dot{\mathbb{R}}^2 = \mathbb{R}^2 \backslash \{\mathbf{0}\}$.

Further, in view of (42),

$$\begin{aligned}\mathcal{C}^\top \circ \mathrm{WF}_{\mathrm{supp}(Fu)}(\mathbb{1}_A) = \big\{(\boldsymbol{x}, \xi) \in \Omega \times \dot{\mathbb{R}}^2 : \exists (s, 2/3) \in \mathrm{supp}(Fu),\, \boldsymbol{x} \in \mathcal{I}(s, 2/3),\\ \boldsymbol{x}^\top \Theta(s)^\perp = 0,\, \xi = \omega\Theta(s),\, \omega \in \dot{\mathbb{R}}\big\}\\ = \big\{\big((2/3)\Theta(s), \omega\Theta(s)\big) \in \Omega \times \dot{\mathbb{R}}^2 :\ (s, 2/3) \in \mathrm{supp}(Fu),\, \omega \in \dot{\mathbb{R}}\big\}. \quad (53)\end{aligned}$$

The set (53) is an arc of $\mathrm{Bd}(B_{2/3}(\mathbf{0}))$ which consists of all points in $\mathrm{Bd}(B_{2/3}(\mathbf{0}))$ whose tangents intersect I^2, that is the closed quarter circle with radius $r = 2/3$ in the first quadrant. This arc is clearly visible in both images of Figure 3. It is an object independent artifact.

Of the terms in (37) the only one that does not depend on $\mathrm{WF}(Fu)$ is $\mathcal{C}_A^\top \circ \mathrm{WF}(\mathbb{1}_A)$. Therefore, the singularities in $\mathcal{C}_A^\top \circ \mathrm{WF}(\mathbb{1}_A)$ can give object independent artifacts in (37). However, the other limited data artifacts are object dependent because they depend on $\mathrm{WF}(Fu)$. Since the Radon line transform satisfies the Bolker condition, there are no Bolker artifacts.

The endpoints of this circular arc are $(0, 2/3)$ and $(2/3, 0)$, and our calculation shows that $(0, 2/3, 0, \omega)$ and $(2/3, 0, 0, \omega)$ for $\omega \in \dot{\mathbb{R}}$ are part of this object independent microlocal artifact. Combining with the object dependent artifacts above the lines $\mathcal{I}(0, 2/3)$ and $\mathcal{I}(\pi/2, 2/3)$, we see there can be artifacts above every point along these lines. This example shows that some points in Y can generate both object dependent and object independent artifacts, as we will discuss in Remark C.5.

Since the Bolker condition holds, the set $\mathcal{C}^\top \circ \mathrm{WF}_A(Fu)$ includes only visible singularities of u. In fact,

$$\mathcal{C}^\top \circ \mathrm{WF}_A(Fu) \subset \big\{(\boldsymbol{x}, \xi) \in \mathrm{WF}(u) : \exists (s, t) \in A(\boldsymbol{x}, \xi) \in \dot{N}^*(\mathcal{I}(s, t))\big\},$$

that is, the singularity $(\boldsymbol{x}, \xi)$ of u is in $\mathcal{C}^\top \circ \mathrm{WF}_A(Fu)$ if ξ is conormal at $\boldsymbol{x}$ to a line of integration that intersects the ROI. Since all four boundary edges of I^2 are part of straight lines hitting the ROI, they are all visible in $\mathrm{Id}_{2/3}u$, even the two edges outside the ROI (Figure 3

left). In contrast to the situation on the right image of Figure 3: Here u is the indicator function of a rotated version of I^2 (rotated by $\pi/4$ around its center). The tangent to the upper right boundary edge does not intersect the ROI. This edge is therefore invisible.

Because R^* satisfies the Bolker condition, all of the covectors found above are in $\mathrm{WF}(\mathcal{L}u)$.

A characterization of artifacts when the angular variable s of the Radon transform is restricted (limited angle problem) is given in [11].

4.3. **Seismic imaging.** In geophysical exploration, the operator F as defined in (16) occurs by the linearization of the underlying nonlinear seismic inverse problem where the symbol H and the function Φ are implicitly given as solutions of two PDEs, see, e.g., [44, 17] and also [6, Appendix E].

Now we describe the situation in more detail. Let

$$X = \{\boldsymbol{x} \in \mathbb{R}^2 : \ x_2 > 0\}$$

be the propagation medium for the waves which are initiated at sources $\boldsymbol{x_s}$ located at $\mathrm{Bd}(X)$ ($x_2 > 0$ is the depth variable and points downwards). The reflected wave fields are recorded by receivers $\boldsymbol{x_r}$ which are located at $\mathrm{Bd}(X)$ as well. Assume that we want to reconstruct the pressure wave speed ν_{pr} from the recordings. In the acoustic regime and for a constant bulk density, the linearization ansatz

$$\frac{1}{\nu_{\mathrm{pr}}^2} = \frac{1+u}{v^2}$$

about the known background velocity model[7] v, leads to the inverse problem $Fu = g$ where g are the processed recordings.

To express F in the format of (15), we parameterize pairs of source and receiver positions by the common offset scanning geometry, that is,

$$\boldsymbol{x_s} = \boldsymbol{x_s}(s) = (s-\alpha, 0)^\top \quad \text{and} \quad \boldsymbol{x_r} = \boldsymbol{x_r}(s) = (s+\alpha, 0)^\top,$$

where $2\alpha \geq 0$ is the common offset and s is in an open subset $\mathtt{S} \subset \mathbb{R}$. Then, we have that

$$H(s, \boldsymbol{x}) = \frac{a(\boldsymbol{x}, \boldsymbol{x_s}(s))a(\boldsymbol{x}, \boldsymbol{x_r}(s))}{v^2(\boldsymbol{x})}, \qquad \varphi(s, \boldsymbol{x}) = \tau(\boldsymbol{x}, \boldsymbol{x_s}(s)) + \tau(\boldsymbol{x}, \boldsymbol{x_r}(s)),$$

where $\tau(\boldsymbol{x}, \boldsymbol{y})$ denotes the travel time of the wave from $\boldsymbol{x} \in X$ to $\boldsymbol{y} \in X$ and it can be computed from the eikonal equation

$$|\mathrm{d}_{\boldsymbol{x}}\tau(\cdot, \boldsymbol{y})|^2 = v^{-2}(\cdot), \quad \tau(\boldsymbol{y}, \boldsymbol{y}) = 0. \tag{54}$$

The amplitude a is the solution of the transport equation

$$\mathrm{div}_{\boldsymbol{x}}\big(a^2(\cdot, \boldsymbol{y})\mathrm{d}_{\boldsymbol{x}}\tau(\cdot, \boldsymbol{y})\big) = 0, \quad \lim_{\boldsymbol{x}\to\boldsymbol{y}} a(\boldsymbol{x}, \boldsymbol{y})|\boldsymbol{x}-\boldsymbol{y}|^{1/2} = \frac{\sqrt{v(\boldsymbol{y})}}{2\sqrt{2\pi}}.$$

Note that F integrates u along reflection isochrones as $\mathcal{I}(s,t)$ contains all points of X which have the travel time t to source $\boldsymbol{x_s}(s)$ and receiver $\boldsymbol{x_r}(s)$.

In general, neither τ nor a is known explicitly but can be computed numerically, see, e.g., [16, 37]. There is an exception: the affine velocity model

$$v(\boldsymbol{x}) = \mathrm{m}x_2 + \mathrm{b} \quad \text{for } \mathrm{m} \geq 0 \text{ and } \mathrm{b} > 0.$$

[7]The velocity model is assumed to satisfy the geometric optics assumption, that is, any two points in X can be connected by a unique ray of geometric optics. Rays are the characteristic curves of the eikonal equation (54).

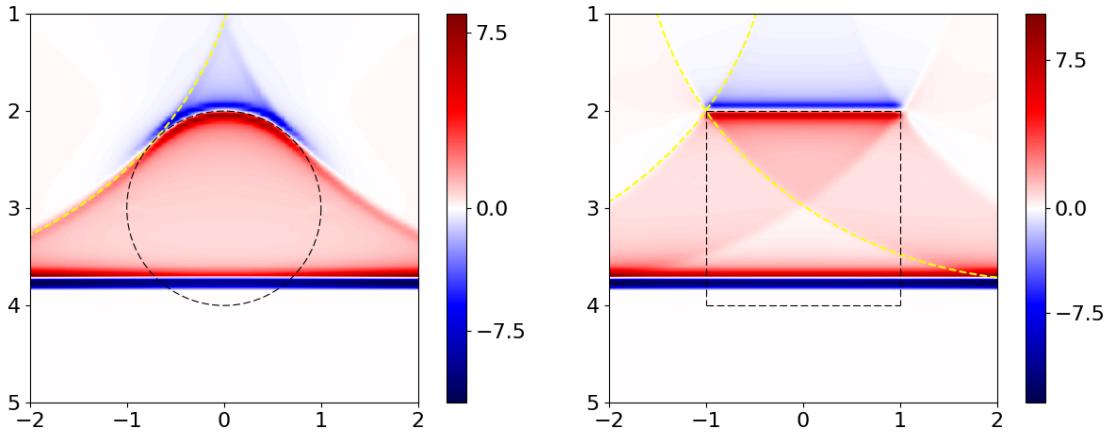

FIGURE 4. Numerical approximation of $\Lambda_A u$ for the velocity model $v(\cdot) = 1$ and the offset $\alpha = 2$ where $u = \mathbb{1}_{B_1((0,3))}$ (left) and $u = \mathbb{1}_{[-1,1]\times[2,4]}$ (right). The black dashed curves indicate the singular support of u and the yellow dashed curves show the predicted limited artifact curves in the left part of both images. Due to axial symmetry with respect to $x_1 = 0$, mirrored versions of these artifact curves also appear in the right part (but are not highlighted by an added colored curve). The straight line at $x_2 = 3.75$ is an object independent artifact.

Explicit expressions for τ and a can be found in, e.g., [28]. It can be shown, see [15, Section 3.1], that $F\colon \mathcal{E}'(\mathcal{X}) \to \mathcal{D}'(\mathbb{R} \times (2\alpha, \infty))$ is an FIO of order $-1/2$ where

$$\mathcal{X} = \operatorname{int}\{\boldsymbol{x} \in X : \forall s \in \mathbb{S} : \mathrm{d}_{\boldsymbol{x}}\varphi(s, \boldsymbol{x}) \neq \mathbf{0}\}.$$

For $\mathrm{m} = 0$ or $\alpha = 0$ the Bolker condition (12) holds in $X = \mathcal{X}$, see [9] and [28], respectively.

4.3.1. *The constant velocity model.* Let us first consider the constant case: $\mathrm{m} = 0$ and $\mathrm{b} = 1$, that is, $v(\cdot) = 1$, $\tau(\boldsymbol{x}, \boldsymbol{y}) = |\boldsymbol{x} - \boldsymbol{y}|$, and $a(\boldsymbol{x}, \boldsymbol{y}) = 1/\big(2\sqrt{2\pi\,\tau(\boldsymbol{x}, \boldsymbol{y})}\big)$. The isochrones $\mathcal{I}(s, t)$, $t > 2\alpha$, are ellipses with foci $\boldsymbol{x_s}(s)$ and $\boldsymbol{x_r}(s)$.[8] No Bolker artifacts will emerge as the Bolker condition holds.

For $s_{\max} = 4.5$, $t_{\min} = 5.5$, and $t_{\max} = 8.5$ let

$$\Lambda_A = -\Delta_{\boldsymbol{x}} F_W^{\dagger} \mathbb{1}_A F, \quad A = [-s_{\max}, s_{\max}] \times [t_{\min}, t_{\max}], \tag{55}$$

be the limited data reconstruction operator. Here, $-\Delta_{\boldsymbol{x}}$ is the Laplace operator and we use the weight

$$W(s, \boldsymbol{x}) = \frac{\left|\det \begin{pmatrix} \mathrm{d}_{\boldsymbol{x}}\varphi(s, \boldsymbol{x}) \\ \partial_s \mathrm{d}_{\boldsymbol{x}}\varphi(s, \boldsymbol{x}) \end{pmatrix}\right|}{H(s, \boldsymbol{x})\,|\mathrm{d}_{\boldsymbol{x}}\varphi(s, \boldsymbol{x})|} \tag{56}$$

which has been suggested in [15, Section 3.2]. For this example, the offset is $\alpha = 2$.

The artifacts occurring in $\Lambda_A u$ for $u = \mathbb{1}_{B_1(\boldsymbol{x}_c)}$, $\boldsymbol{x}_c = (0, 3)$, and $u = \mathbb{1}_{[-1,1]\times[2,4]}$, see Figure 4, can be fully explained by our theory. In fact, we observe an object independent artifact which is the straight line at $x_2 = 3.75$ in both images of Figure 4. It is an element of the set $\mathcal{C}^{\top} \circ \mathrm{WF}_{\operatorname{supp}(Fu)}(\mathbb{1}_A)$, see (42), which we will now demonstrate.

[8] For $\alpha = 0$, F is a variant the spherical Radon transform of Section 4.1 where the centers of the spheres are on a line.

The singularities in $\mathrm{WF}_{\mathrm{supp}(Fu)}(\mathbb{1}_A)$ with $\eta_2 \neq 0$ are in the set

$$\big\{((s,t_{\max}),(0,\eta_2)) : s \in (-s_{\max}, s_{\max}),\ \eta_2 \in \dot{\mathbb{R}}\big\}$$
$$\cup \big\{((-s_{\max},t_{\max}),\eta) : \eta \in \mathbb{R}^2,\ \eta_2 \in \dot{\mathbb{R}}\big\} \cup \big\{((s_{\max},t_{\max}),\eta) : \eta \in \mathbb{R}^2,\ \eta_2 \in \dot{\mathbb{R}}\big\}$$

since the other horizontal edge of $\mathrm{Bd}(A)$ does not intersect $\mathrm{supp}(Fu)$. The base points $\boldsymbol{x}$ of singularities in $\mathcal{C}^\top \circ \mathrm{WF}_{\mathrm{supp}(Fu)}(\mathbb{1}_A)$ are thus located on $\mathcal{I}(s,t_{\max})$ satisfying $\partial_s\varphi(s,\boldsymbol{x}) = 0$, $s \in [-s_{\max}, s_{\max}]$. To solve this equation for $\boldsymbol{x}$ we provide the derivative

$$\partial_s\varphi(s,\boldsymbol{x}) = \frac{s - x_1 - \alpha}{|\boldsymbol{x} - \boldsymbol{x_s}(s)|} + \frac{s - x_1 + \alpha}{|\boldsymbol{x} - \boldsymbol{x_r}(s)|}$$

and the parameterization

$$\mathcal{I}(s,t_{\max}) = \big\{\gamma_s(\vartheta) : \vartheta \in [0,\pi]\big\}, \quad \gamma_s(\vartheta) = \left(s + \frac{t_{\max}}{2}\cos\vartheta, \sqrt{\frac{t_{\max}^2}{4} - \alpha^2}\,\sin\vartheta\right).$$

The function $[0,\pi] \ni \vartheta \mapsto \partial_s\varphi(s,\gamma_s(\vartheta))$ is decreasing[9] and has its only zero at $\vartheta = \pi/2$ yielding the base point $\gamma_s(\pi/2) = (s, \sqrt{t_{\max}^2/4 - \alpha^2}) = (s, 3.75)$ for each $s \in [-s_{\max}, s_{\max}]$ with corresponding vertical covectors $\xi = (0,\xi_2)$, $\xi_2 \in \dot{\mathbb{R}}$. Hence, the base points in $\mathcal{C}^\top \circ \mathrm{WF}_B(\mathbb{1}_A)$ form a horizontal line at $x_2 = 3.75$.

Since the Bolker condition holds, the set $\mathcal{C}^\top \circ \mathrm{WF}_A(Fu)$, see (38), contains only visible singularities. Those are wave fronts $(\boldsymbol{x},\xi) \in \mathrm{WF}(u)$ such there is an isochrone $\mathcal{I}(s,t)$ for $(s,t) \in A$ such that $(\boldsymbol{x},\xi) \in N^*(\mathcal{I}(s,t))$ As a consequence we only see a small part of the singular support of u: In the left image of Figure 4, only a polar cap is visible around the North Pole, while in the right image, we can see the upper edge of the square, but not the vertical and lower edges.

Finally, limited data artifacts can be observed which are in the set

$$\big(\mathcal{C}^\top \circ M^{\mathrm{c}}(A,u)\big) \cup \big(\mathcal{C}^\top \circ M^{\mathrm{nc}}(A,u)\big)\,, \tag{57}$$

see Section 3.6.1. Those are above ellipses $\mathcal{I}(s,t)$ for $(s,t) \in \mathrm{Bd}(A)$ satisfying $\mathrm{WF}_{(s,t)}(Fu) \neq \emptyset$. In the case of $u = \mathbb{1}_{B_1(\boldsymbol{x}_c)}$, we have that $\mathrm{WF}_{(\pm s_{\max},t)}(Fu) = \emptyset$ for all $t \in [t_{\min}, t_{\max}]$, as for these t, $\mathcal{I}(\pm s_{\max}, t)$ is disjoint from the closure of $B_1(\boldsymbol{x}_c)$. Also $\mathrm{WF}_{(s,t_{\min})}(Fu) = \emptyset$ for $s \in [-s_{\max}, s_{\max}]$. Hence, it remains to investigate pairs $(s,t_{\max})$, $s \in [-s_{\max}, s_{\max}]$. Only the two ellipses $\mathcal{I}(s_\pm, t_{\max})$ for $s_\pm \approx \pm 4.07$ are tangent to $\mathrm{Bd}(B_1(\boldsymbol{x}_c))$ and thus occur as limited data artifacts in the left image of Figure 4. Note that we do not need to calculate $M^{\mathrm{nc}}(A,u)$ and $M^{\mathrm{c}}(A,u)$ separately in (57); as noted in Remark C.4, we just need to find the singularities above all points $(s,t) \in B_2 = \mathrm{sing\,supp}(Fu) \cap \mathrm{sing\,supp}(\mathbb{1}_A)$.

The situation is a little bit different for $u = \mathbb{1}_{[-1,1]\times[2,4]}$. Again, Fu has no wave fronts above $(s,t_{\min})$, $s \in [-s_{\max}, s_{\max}]$, since none of the corresponding isochrones hit the square. All isochrones with parameters $(s,t_{\max})$, $s \in [-s_{\max}, s_{\max}]$, intersect the edges of the square transversally. In view of Proposition 3.4, there are no wave fronts above these intersection points. However, there are two ellipses with parameters $(s_\pm, t_{\max})$, $s_\pm = \pm(1 - 17\sqrt{161}/60) \approx \pm 2.595$, which intersect the square at its upper left and right corners. Since each vector in $\dot{\mathbb{R}}^2$ is a covector above the corners, the ellipses $\mathcal{I}(s_\pm, t_{\max})$ show up as artifact curves in the right image of Figure 4. Further, the ellipses $\mathcal{I}(\pm s_{\max}, t_{\mathrm{cor}})$, $t_{\mathrm{cor}} = 2.5 + \sqrt{34.25} \approx 8.352$, pass through the upper corners as well and give rise to corresponding limited data artifacts. So we have two artifact curves hitting each upper corner.

[9] This can be seen by taking the derivative with respect to ϑ which is negative on $(0,\pi)$.

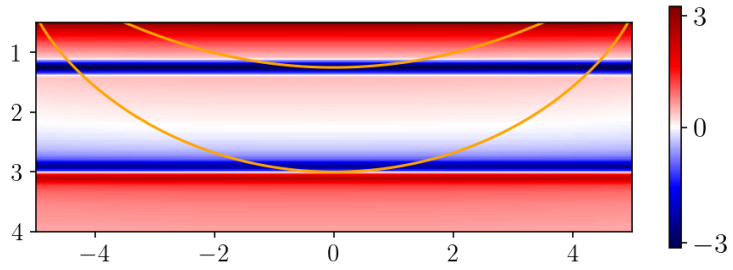

FIGURE 5. Numerical approximation of $\Lambda_A u$, see (55) and (56), for the velocity model $v(\mathbf{x}) = 0.1x_2 + 0.5$ and the offset $\alpha = 5$ where $u = \mathbb{1}_{x_2 \geq 3}$ is the indicator function of a half space. The horizontal line at about $x_2 = 1.25$ is a mirror artifact caused by the shape of isochrones which are tangent to the line $x_2 = 3$. The orange curve is one representative of those isochrones restricted to the selected reconstruction area.

4.3.2. *The linearly increasing velocity model.* Now, let $v(\boldsymbol{x}) = \mathrm{m}x_2 + \mathrm{b}$ with $\mathrm{m} > 0$ and $\mathrm{b} > 0$. Here, the Bolker condition is not satisfied in X but in

$$\mathcal{X} = \{\boldsymbol{x} \in X : x_2 > x_{\min}\} \quad \text{and} \quad Y = \mathbb{S} \times (t_{\text{first}}, \infty)$$

where

$$x_{\min} = \frac{\mathrm{b}}{\mathrm{m}} \left(\sqrt{1 + \frac{\mathrm{m}^2\alpha^2}{\mathrm{b}^2}} - 1 \right), \quad t_{\text{first}} = \frac{2}{\mathrm{m}} \operatorname{asinh}\left(\frac{\mathrm{m}\,\alpha}{\mathrm{b}} \right),$$

see [28]. The geometry of the isochrones yields mirror artifacts, and this configuration is an example of Case II in Section 3.8. Even though there is no explicit analytic representation of $\mathcal{I}(s,t)$ known, the authors of [28] identified exactly two points on $\mathcal{I}(s,t)$, namely $(s, p_\pm)$ with

$$p_\pm = \frac{\mathrm{b}}{\mathrm{m}} \left(\cosh \frac{\mathrm{m}t}{2} - 1 \right) \pm \sqrt{\frac{\mathrm{b}^2}{\mathrm{m}^2} \sinh^2 \frac{\mathrm{m}t}{2} - \alpha^2} \quad \text{for} \quad t > t_{\text{first}},$$

at which $\mathcal{I}(s,t)$ has a horizontal tangent at $(s, p_\pm)$. As a consequence the equation $\partial_s \varphi(0, \cdot) = 0$ has the two solutions $(s, p_\pm)$. For

$$t < \underline{t} = \frac{4}{\mathrm{m}} \operatorname{asinh}\left(\frac{\mathrm{m}}{\mathrm{b}} \frac{\alpha}{2} \right)$$

the values for p_- and p_+ are positive and, due to (38) and (45), a mirror artifact might form in $\Lambda_A u$ above (x_1, p_-) provided u has wave fronts above (x_1, p_+) with vertical covectors, see (55) and (56) for the definition of Λ_A.

For a concrete example, set $\mathrm{m} = 0.1$, $\mathrm{b} = 0.5$, and $\alpha = 5$. Then, $t_{\text{first}} \approx 17.6275$, $x_{\min} \approx 2.0711$, and $\underline{t} \approx 19.2485$. Further, $u = \mathbb{1}_{x_2 \geq 3}$ is the indicator function of a half space. Isochrones $\mathcal{I}(s, t_3)$ with $t_3 \approx 17.8416 < \underline{t}$ are tangent to the line $x_2 = p_+ = 3$, see the orange curve in Figure 5. Thus, the horizontal line artifact we observe in $\Lambda_A u$ at $x_2 = p_- \approx 1.25$ in Figure 5, is a mirror artifact. Please note that the limited data set used $A = [-12, 12] \times [17.633, 47.633]$ was chosen so large that no other artifacts are present in the displayed image section.

A more exciting pattern of mirror artifacts forms in $\Lambda_A u$, when u is the indicator function of a half space which is confined by a periodic curve, see Figure 6. Please note that we cannot analytically describe this pattern since no explicit expression for the isochrones is known. However, each artifact curve must be tangent to the corresponding isochrone at its mirror point for the following reason. If $(\boldsymbol{x}, \xi)$ is a mirror artifact, then $(\boldsymbol{x}, \xi)$ is conormal to its isochrone

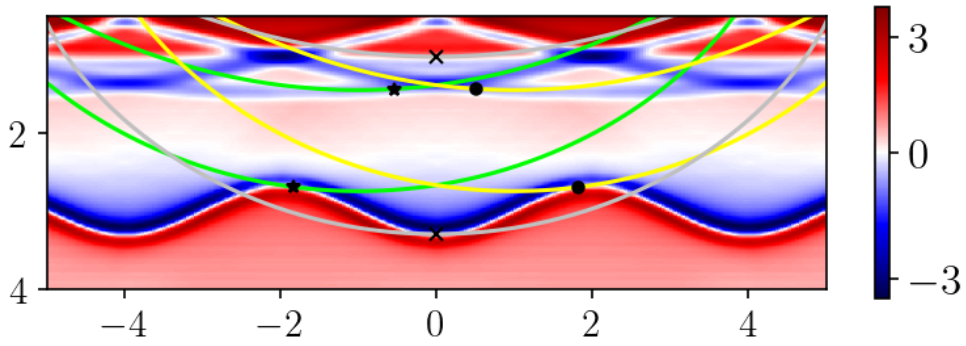

FIGURE 6. Numerical approximation of $\Lambda_A u$ for $u = \mathbb{1}_{x_2 \geq 3+0.3\cos(\pi x_1/2)}$. The other settings are as in Figure 5. The three plotted curves are isochrones for different source/receiver pairs. They touch the singular support of u at three different points, which are mirrored to points on the respective isochrone touching the artifact curve, see (38). These points are marked by black dots (yellow isochrone), black asterisks (green isochrone), and black crosses (light gray isochrone).

by Proposition 3.4. Since the artifact curve is caused by these mirror artifacts, $(\boldsymbol{x}, \xi)$ is conormal to the artifact curve, too (the wavefront set of such singularities on curves is the conormal bundle of the curve). This fact underpins the visual determination of the three mirror points indicated in Figure 6.

All computations in this subsection have been done using Python routines available from [14].

APPENDIX A. GENERAL CALCULATIONS

We now give a few basic statements we will use throughout the appendix. The notation used here was introduced in Sections 2 and 3.

Proposition A.1. *Let $u \in L^1_c(X, \mathbb{R})$ and $(\boldsymbol{x}_0, \xi_0) \in \mathrm{WF}(u)$. Let $D \subset Y$. Then the following are equivalent*

(i) $\mathcal{C}_D \circ \{(\boldsymbol{x}_0, \xi_0)\} \neq \emptyset$.
(ii) *There is a $(\boldsymbol{s}_0, t_0) \in D$ such that $(\boldsymbol{x}_0, \xi_0) \in N^*(\mathcal{I}(\boldsymbol{s}_0, t_0)) \cap \mathrm{WF}(u)$.*
(iii) *There is a $(\boldsymbol{s}_0, t_0, \omega_0) \in D \times \dot{\mathbb{R}}$ such that $\boldsymbol{x}_0 \in \mathcal{X}(\boldsymbol{s}_0, t_0, u)$ and $\xi_0 = \omega_0 \, \mathrm{d}_{\boldsymbol{x}} \varphi(\boldsymbol{s}_0, \boldsymbol{x}_0)$.*

In this case,

$$\mathcal{C}_D \circ \{(\boldsymbol{x}_0, \xi_0)\} = \big\{(\boldsymbol{s}_0, t_0, -\omega_0 \, \mathrm{d}_{\boldsymbol{s}} \varphi(\boldsymbol{s}_0, \boldsymbol{x}_0), \omega_0) : \ (\boldsymbol{s}_0, t_0, \omega_0) \in D \times \dot{\mathbb{R}}, \\ \boldsymbol{x}_0 \in \mathcal{X}(\boldsymbol{s}_0, t_0, u), \xi_0 = \omega_0 \, \mathrm{d}_{\boldsymbol{x}} \varphi(\boldsymbol{s}_0, \boldsymbol{x}_0)\big\}. \tag{58}$$

If $\boldsymbol{x}_0 \in X$ and $(\boldsymbol{s}, t) \in Y$, then

$$\boldsymbol{x}_0 \in \mathcal{X}(\boldsymbol{s}, t, u) \implies \forall \omega \in \dot{\mathbb{R}}, \ (\boldsymbol{s}, t, -\omega \, \mathrm{d}_{\boldsymbol{s}} \varphi(\boldsymbol{x}, \boldsymbol{x}_0), \omega) \in \mathcal{C} \circ \mathrm{WF}(u), \tag{59}$$

and $\mathcal{X}(\boldsymbol{s}, t, u)$ contains base points of all covectors in $N^*(\mathcal{I}(\boldsymbol{s}, t)) \cap \mathrm{WF}(u)$.

This proposition explains the statements about $\mathcal{X}(\boldsymbol{s}, t, u)$ and the implication in (25) at the start of Section 3.3 and provides further perspective on the set $\mathcal{X}(\boldsymbol{s}, t, u)$.

Proof of Proposition A.1 . Let $D \subset Y$. Then by (18) and (20), $\mathcal{C}_D$ is the set of all

$$(\boldsymbol{s}_0, t_0, -\omega_0 \, \mathrm{d}_{\boldsymbol{s}} \varphi(\boldsymbol{s}_0, \boldsymbol{x}_0), \omega_0; \boldsymbol{x}_0, \omega_0 \, \mathrm{d}_{\boldsymbol{x}} \varphi(\boldsymbol{s}_0, \boldsymbol{x}_0))$$
$$\text{where} \tag{60}$$
$$(\boldsymbol{s}_0, t_0, \omega_0) \in D \times \dot{\mathbb{R}}, \ \boldsymbol{x}_0 \in \mathcal{I}(\boldsymbol{s}_0, t_0).$$

This implies the following. Let $(\boldsymbol{x}_0, \xi_0) \in T^*(X)$. Then, $\mathcal{C}_D \circ \{(\boldsymbol{x}_0, \xi_0)\} \neq \emptyset$ if and only if there is a $(\boldsymbol{s}_0, t_0, \omega_0) \in D \times \dot{\mathbb{R}}$ such that

$$(\boldsymbol{s}_0, t_0, -\omega_0 \, \mathrm{d}_{\boldsymbol{s}} \varphi(\boldsymbol{s}_0, \boldsymbol{x}_0), \omega_0; \boldsymbol{x}_0, \xi_0) \in \mathcal{C}_D$$

by the definition of composition of sets. This can hold if and only if $(\boldsymbol{s}_0, t_0) \in D$, $\boldsymbol{x}_0 \in \mathcal{I}(\boldsymbol{s}_0, t_0)$, and $\xi_0 = \omega_0 \, \mathrm{d}_{\boldsymbol{x}} \varphi(\boldsymbol{s}_0, \boldsymbol{x}_0)$ for some $\omega_0 \in \dot{\mathbb{R}}$.

Therefore, if $(\boldsymbol{x}_0, \xi_0) \in \mathrm{WF}(u)$, then (i) implies (iii) since $(\boldsymbol{x}_0, \, \mathrm{d}_{\boldsymbol{x}} \varphi(\boldsymbol{s}, \boldsymbol{x}_0)) \in \mathrm{WF}(u)$ if and only if $\forall \omega_0 \in \dot{\mathbb{R}}$, $(\boldsymbol{x}_0, \omega_0 \, \mathrm{d}_{\boldsymbol{x}} \varphi(\boldsymbol{s}, \boldsymbol{x}_0)) \in \mathrm{WF}(u)$. Assertion (ii) is a different way of writing (iii).

Now we show (iii) implies (i). Assume there is a $(\boldsymbol{s}_0, t_0, \omega_0) \in D \times \dot{\mathbb{R}}$ such that $\boldsymbol{x}_0 \in \mathcal{X}(\boldsymbol{s}_0, t_0, u)$ and $\xi_0 = \omega_0 \, \mathrm{d}_{\boldsymbol{x}} \varphi(\boldsymbol{s}_0, t_0)$. As u is real-valued, $(\boldsymbol{x}_0, \xi_0) \in \mathrm{WF}(u)$, and (60) shows that $\mathcal{C}_D \circ \{(\boldsymbol{x}_0, \xi_0)\} \neq \emptyset$.

Proofs of the last two statements in the proposition follow from the arguments we have provided and are left to the reader. □

Appendix B. Proofs of the statements in Section 3.3 about $\mathbb{1}_A Fu$

Proposition B.1. *Let $D \subset Y$. Then,*

$$\begin{aligned} \mathrm{WF}_D(Fu) \subset \mathcal{C}_D \circ \mathrm{WF}(u) = & \bigcup_{\substack{(\boldsymbol{s},t) \in D \\ \mathcal{X}(\boldsymbol{s},t,u) \neq \emptyset}} \{(\boldsymbol{s}, t, -\omega \, \mathrm{d}_{\boldsymbol{s}} \varphi(\boldsymbol{s}, \boldsymbol{x}_0), \omega) : \ \boldsymbol{x}_0 \in \mathcal{X}(\boldsymbol{s}, t, u), \\ & \qquad\qquad\qquad\qquad\qquad\qquad\qquad\qquad \omega \in \dot{\mathbb{R}}\} \\ =: & \, M^{\mathrm{F}}(D, u). \end{aligned} \tag{61}$$

Proof. By the Hörmander-Sato lemma, (11), $\mathrm{WF}_D(Fu) \subset \mathcal{C}_D \circ \mathrm{WF}(u)$. To calculate $\mathcal{C}_D \circ \mathrm{WF}(u)$, we let $(\boldsymbol{x}_0, \xi_0) \in \mathrm{WF}(u)$ and use Proposition A.1. For the composition to be nonempty, for some $(\boldsymbol{s}, t) \in D$, $\boldsymbol{x}_0 \in \mathcal{X}(\boldsymbol{s}, t, u)$ and for some $\omega_0 \in \dot{\mathbb{R}}$, $\xi_0 = \omega_0 \, \mathrm{d}_{\boldsymbol{x}} \varphi(\boldsymbol{s}, \boldsymbol{x}_0)$. In this case, $\mathcal{C}_D \circ \{(\boldsymbol{x}_0, \xi_0)\}$ is the set of all $(\boldsymbol{s}, t, -\omega_0 \, \mathrm{d}_{\boldsymbol{x}} \varphi(\boldsymbol{s}, \boldsymbol{x}_0), \omega_0)$ such that $(\boldsymbol{s}, t, \omega_0) \in D \times \dot{\mathbb{R}}$, $\boldsymbol{x}_0 \in \mathcal{X}(\boldsymbol{s}, t, u)$, and $\xi_0 = \omega_0 \, \mathrm{d}_{\boldsymbol{x}} \varphi(\boldsymbol{s}, \boldsymbol{x}_0)$ by (58).

However, because u is real-valued, if $\boldsymbol{x}_0 \in \mathcal{X}(\boldsymbol{s}, t, u)$, then for any $\omega \in \dot{\mathbb{R}}$,

$$(\boldsymbol{x}_0, \omega \, \mathrm{d}_{\boldsymbol{x}} \varphi(\boldsymbol{s}, \boldsymbol{x}_0)) \in N^*(\mathcal{I}(\boldsymbol{s}, t)) \cap \mathrm{WF}(u).$$

Therefore, whenever $\mathcal{X}(\boldsymbol{s}, t, u) \neq \emptyset$, and for any $\boldsymbol{x}_0 \in \mathcal{X}(\boldsymbol{s}, t, u)$ and $\omega \in \dot{\mathbb{R}}$,

$$(\boldsymbol{s}, t, -\omega \, \mathrm{d}_{\boldsymbol{s}} \varphi(\boldsymbol{s}, \boldsymbol{x}_0), \omega) \in \mathcal{C}_D \circ \mathrm{WF}(u). \tag{62}$$

Then, $M^{\mathrm{F}}(D, u)$ is the set of all covectors $(\boldsymbol{s}, t, -\omega \, \mathrm{d}_{\boldsymbol{x}} \varphi(\boldsymbol{s}, \boldsymbol{x}_0), \omega)$ for all $\boldsymbol{x}_0 \in \mathcal{X}(\boldsymbol{s}, t, u)$ and $\omega \in \dot{\mathbb{R}}$ when $(\boldsymbol{s}, t) \in D$ and $\mathcal{X}(\boldsymbol{s}, t, u) \neq \emptyset$. This finishes the proof. □

Singularities of $\mathbb{1}_A Fu$ above $\mathrm{Bd}(A)$. To analyze the interaction of singularities of $\mathbb{1}_A$ with those of Fu, we will use Corollary 2.5, which describes the wave front sets of products of functions. Please refer to (31) for the definition of B, B_2, B_2^{c}, and B_2^{nc}. Then B is the largest subset of $\mathrm{Bd}(A)$ on which $\mathbb{1}_A Fu$ can have a singularity and B_2 is the set of points above which *both* $\mathbb{1}_A$ and Fu have singularities. The set B_2^{c} is the set of base points where non-cancellation condition of Corollary 2.5 part (ii) fails, and B_2^{nc} is the set of base points where this condition holds.

We now justify (33). As explained in Section 3.3, we will take the largest set of possible singularities of the function $\mathbb{1}_A Fu$ above $(\boldsymbol{s}, t)$, which is $\dot{T}^*_{(\boldsymbol{s},t)}(Y)$, because $\mathrm{WF}_{(\boldsymbol{s},t)}(\mathbb{1}_A Fu)$ is always a subset of $T^*_{(\boldsymbol{s},t)}(Y)$.

Proposition B.2. *The largest possible set of singularities of $\mathbb{1}_A Fu$ above points in B_2^{c} (at which the local non-cancellation condition (ii) fails) is*

$$T^*_{B_2^{\mathrm{c}}}(Y) = \left\{(\boldsymbol{s},t,\eta)\in \dot{T}^*(Y):\ (\boldsymbol{s},t)\in B_2^{\mathrm{c}}\right\} \tag{63}$$

$$\subset \bigcup_{(\boldsymbol{s},t)\in A} \big\{(\boldsymbol{s},t,\eta)\in \dot{T}^*(Y):\ \exists \boldsymbol{x}_0\in \mathcal{X}(\boldsymbol{s},t,u),\ (\boldsymbol{s},t,-\mathrm{d}_{\boldsymbol{s}}\varphi(\boldsymbol{s},\boldsymbol{x}_0),1)\in \mathrm{WF}(\mathbb{1}_A)\big\} \tag{64}$$

$$=: M^{\mathrm{c}}(A,u).$$

If one knows B_2^{c}, then one should use equation (63), and if not, one can use (64) in (36).

Proof. By (62), if $(\boldsymbol{s},t)\in A$ and $\boldsymbol{x}_0\in\mathcal{X}(\boldsymbol{s},t,u)$, then

$$(\boldsymbol{s},t,-\omega\,\mathrm{d}_{\boldsymbol{s}}\varphi(\boldsymbol{s},\boldsymbol{x}_0),\omega)\in \mathcal{C}_A\circ\mathrm{WF}(u)\ \ \forall\omega\in\dot{\mathbb{R}}.$$

Since $\mathcal{C}_A\circ\mathrm{WF}(u)$ contains $\mathrm{WF}_A(Fu)$, every $(\boldsymbol{s},t,\eta)\in\mathrm{WF}(\mathbb{1}_A)\cap\mathrm{WF}(Fu)$ is of this form. By setting $\omega=1$, we see $(\boldsymbol{s},t,-\mathrm{d}_{\boldsymbol{s}}\varphi(\boldsymbol{s},\boldsymbol{x}_0),1)\in\mathrm{WF}(\mathbb{1}_A)$. This justifies the containment. □

Proposition B.3. *The set of added singularities given by Corollary 2.5 part (ii) is contained in the set in (65), and*

$$\left\{(\boldsymbol{s},t,\eta+\nu)\in\dot{T}^*(Y):\ (\boldsymbol{s},t)\in B_2^{\mathrm{nc}},\eta\in\mathrm{WF}_{(\boldsymbol{s},t)}(\mathbb{1}_A),\ \nu\in\mathrm{WF}_{(\boldsymbol{s},t)}(Fu)\right\} \tag{65}$$

$$\subset \bigcup_{(\boldsymbol{s},t)\in B_2^{\mathrm{nc}}} \big\{(\boldsymbol{s},t,\eta+\nu)\in\dot{T}^*(Y):\ \eta\in\mathrm{WF}_{(\boldsymbol{s},t)}(\mathbb{1}_A),\ \omega\in\dot{\mathbb{R}},\ \boldsymbol{x}_0\in\mathcal{X}(\boldsymbol{s},t,u),\ :\ \nu=(-\omega\,\mathrm{d}_{\boldsymbol{s}}\varphi(\boldsymbol{s},\boldsymbol{x}_0),\omega)\big\} \tag{66}$$

$$=: M^{\mathrm{nc}}(A,u).$$

Proof. If $(\boldsymbol{s},t,\nu)\in\mathrm{WF}(Fu)$, then by (58), $\nu=(-\omega\,\mathrm{d}_{\boldsymbol{s}}\varphi(\boldsymbol{s},\boldsymbol{x}_0),\omega)$ for some $\boldsymbol{x}_0\in\mathcal{X}(\boldsymbol{s},t,u)$. This explains the expression for ν in (66) and finishes the proof. □

To use (66), one needs to know B_2^{nc}, but if it is not known, one can note that

$$B_2^{\mathrm{nc}}\subset\left\{(\boldsymbol{s},t)\in A:\ \forall\boldsymbol{x}_0\in\mathcal{X}(\boldsymbol{s},t,u),\ (\boldsymbol{s},t,-\mathrm{d}_{\boldsymbol{s}}\varphi(\boldsymbol{s},\boldsymbol{x}_0),1)\notin\mathrm{WF}(\mathbb{1}_A)\right\}. \tag{67}$$

This holds using a similar argument to that at the end of the proof of Proposition B.2.

The set in (65) can be larger than the singularities of $\mathbb{1}_A Fu$ above B_2^{nc} because Corollary 2.5 part (ii) is a containment.

Appendix C. Proofs of the statements in section 3.4

We start with the containment for $\mathcal{L}u$: composing $\mathcal{C}_A^\top$ with the right side of (36)

$$\begin{aligned}\mathrm{WF}(\mathcal{L}u)\subset &\left(\mathcal{C}_A^\top\circ M^{\mathrm{F}}(A,u)\right)\cup\left(\mathcal{C}_A^\top\circ M^{\mathrm{c}}(A,u)\right)\cup\left(\mathcal{C}_A^\top\circ M^{\mathrm{nc}}(A,u)\right)\\ &\cup\left(\mathcal{C}_A^\top\circ\mathrm{WF}_{\mathrm{supp}(Fu)}(\mathbb{1}_A)\right).\end{aligned} \tag{68}$$

If B_2^{c} is known, one can replace $M^{\mathrm{F}}(A,u)$ by $T^*_{B_2^{\mathrm{c}}}(Y)$ in calculating (68), as noted below Proposition B.2.

We first prove (38).

Proposition C.1. *For $u\in L^1_c(X,\mathbb{R})$,*

$$\mathcal{C}_A^\top\circ M^{\mathrm{F}}(A,u)=\bigcup_{\substack{(\boldsymbol{s},t)\in A\\ \mathcal{X}(\boldsymbol{s},t,u)\neq\emptyset}}\big\{(\boldsymbol{x},\omega\,\mathrm{d}_{\boldsymbol{x}}\varphi(\boldsymbol{s},\boldsymbol{x})):\ \boldsymbol{x}\in\mathcal{I}(\boldsymbol{s},t),\ \omega\in\dot{\mathbb{R}},\ \boldsymbol{x}_0\in\mathcal{X}(\boldsymbol{s},t,u),\ \mathrm{d}_{\boldsymbol{s}}\varphi(\boldsymbol{s},\boldsymbol{x})=\mathrm{d}_{\boldsymbol{s}}\varphi(\boldsymbol{s},\boldsymbol{x}_0)\big\}.$$

Proof. By Proposition B.1, the arbitrary covector in $M^{\mathrm{F}}(A,u)$ is of the form

$$(\boldsymbol{s},t,-\omega\,\mathrm{d}_{\boldsymbol{s}}\varphi(\boldsymbol{s},\boldsymbol{x}_0),\omega)\ \text{ where }\ (\boldsymbol{s},t)\in A,\ \mathcal{X}(\boldsymbol{s},t,u)\neq\emptyset,\ \boldsymbol{x}_0\in\mathcal{X}(\boldsymbol{s},t,u),\ \omega\in\dot{\mathbb{R}}. \tag{69}$$

To compose with $\mathcal{C}_A^{\top}$ we start with the arbitrary covector in $\mathcal{C}_A^{\top}$,

$$\begin{gathered}(\boldsymbol{x},\omega'\,\mathrm{d}_{\boldsymbol{x}}\varphi(\boldsymbol{s}',\boldsymbol{x});\boldsymbol{s}',t',-\omega'\,\mathrm{d}_{\boldsymbol{s}}\varphi(\boldsymbol{s},'\boldsymbol{x}),\omega')\\ \text{where }\ (\boldsymbol{s}',t')\in A,\ \boldsymbol{x}\in\mathcal{I}(\boldsymbol{s}',t'),\ \omega'\in\dot{\mathbb{R}}.\end{gathered} \tag{70}$$

We equate the $(\boldsymbol{s},t,\eta)$ coordinates of this expression with (69). This shows that $\boldsymbol{s}'=\boldsymbol{s}$, $t'=t$, $\omega'=\omega$, and $\mathrm{d}_{\boldsymbol{s}}\varphi(\boldsymbol{s},\boldsymbol{x})=\mathrm{d}_{\boldsymbol{s}}\varphi(\boldsymbol{s},\boldsymbol{x}_0)$.

Therefore, the arbitrary covector in the composition $\mathcal{C}_A^{\top}\circ M^{\mathrm{F}}(A,u)$ is $(\boldsymbol{x},\omega\,\mathrm{d}_{\boldsymbol{x}}\varphi(\boldsymbol{s},\boldsymbol{x}))$ where $(\boldsymbol{s},t)\in A$, $\mathcal{X}(\boldsymbol{s},t,u)\neq\emptyset$, $\boldsymbol{x}\in\mathcal{I}(\boldsymbol{s},t)$, $\omega\in\dot{\mathbb{R}}$, $\boldsymbol{x}_0\in\mathcal{X}(\boldsymbol{s},t,u)$, and $\mathrm{d}_{\boldsymbol{s}}\varphi(\boldsymbol{s},\boldsymbol{x})=\mathrm{d}_{\boldsymbol{s}}\varphi(\boldsymbol{s},\boldsymbol{x}_0)$. □

We now calculate the composition of the sets in Proposition B.2 with $\mathcal{C}_A^{\top}$ to take care of the second term in (68).

Proposition C.2. *For $u\in L^1_c(X,\mathbb{R})$,*

$$\mathcal{C}_A^{\top}\circ T^*_{B_2^{\mathrm{c}}}(Y)=\bigcup_{(\boldsymbol{s},t)\in B_2^{\mathrm{c}}}\dot{N}^*(\mathcal{I}(\boldsymbol{s},t)), \tag{71}$$

and this set is contained in

$$\begin{aligned}\mathcal{C}_A^{\top}\circ M^{\mathrm{c}}(A,u)=\bigcup_{(\boldsymbol{s},t)\in A}\big\{(\boldsymbol{x},\xi)\in\dot{N}^*(\mathcal{I}(\boldsymbol{s},t)):\ &\exists\boldsymbol{x}_0\in\mathcal{X}(\boldsymbol{s},t,u),\\ &(\boldsymbol{s},t,-\mathrm{d}_{\boldsymbol{s}}\varphi(\boldsymbol{s},\boldsymbol{x}_0),1)\in\mathrm{WF}(\mathbb{1}_A)\big\}.\end{aligned} \tag{72}$$

The set in (72) is the union of all $\dot{N}^*(\mathcal{I}(\boldsymbol{s},t))$ for which u has a singularity conormal to $\mathcal{I}(\boldsymbol{s},t)$ and for which its image under $\mathcal{C}_A$ is in $\mathrm{WF}(\mathbb{1}_A)$.

If one knows B_2^{c}, then one should use equation (71) in (68) to find an upper bound for $\mathrm{WF}(\mathcal{L}u)$, and if not, one can use (72). If $F\colon\mathcal{E}'(X)\to\mathcal{D}'(Y)$ satisfies the Bolker condition, then these sets are equal.

Proof of Proposition C.2. To prove (71), we start with an arbitrary covector in $\mathcal{C}_A^{\top}$ as given by (70) and equate the $(\boldsymbol{s},t,\eta)$ coordinates with the arbitrary covector $(\boldsymbol{s},t,\eta)\in\dot{T}^*(Y)$ where there exists a $\boldsymbol{x}_0\in\mathcal{X}(\boldsymbol{s},t,u)$ such that $(\boldsymbol{s},t,-\mathrm{d}_{\boldsymbol{s}}\varphi(\boldsymbol{s},\boldsymbol{x}_0),1)\in\mathrm{WF}(\mathbb{1}_A)$. Therefore $\boldsymbol{s}'=\boldsymbol{s}$, and $t'=t$, $\omega'=\omega$ and $-\omega\,\mathrm{d}_{\boldsymbol{s}}\varphi(\boldsymbol{s},\boldsymbol{x})=\eta'$. This puts restrictions on η for the composition to be nonempty but not on $\boldsymbol{x}\in\mathcal{I}(\boldsymbol{s},t)$. Since ω is arbitrary, the composition is made up of all $(\boldsymbol{x},\omega\,\mathrm{d}_{\boldsymbol{x}}\varphi(\boldsymbol{s},\boldsymbol{x}))$ for $\boldsymbol{x}\in\mathcal{I}(\boldsymbol{s},t)$, that is all points in $\dot{N}^*(\mathcal{I}(\boldsymbol{s},t))$ for all $(\boldsymbol{s},t)\in A$ for which there exists an $\boldsymbol{x}_0\in\mathcal{X}(\boldsymbol{s},t,u)$ such that $(\boldsymbol{s},t,-\mathrm{d}_{\boldsymbol{s}}\varphi(\boldsymbol{s},\boldsymbol{x}_0),1)\in\mathrm{WF}(\mathbb{1}_A)$. This proves (72). □

We now prove the third composition.

Proposition C.3. *For $u\in L^1_c(X,\mathbb{R})$,*

$$\begin{aligned}\mathcal{C}_A^{\top}\circ M^{\mathrm{nc}}(A,u)=\bigcup_{(\boldsymbol{s},t)\in B_2^{\mathrm{nc}}}\big\{(\boldsymbol{x},(\eta_n+\omega)\,\mathrm{d}_{\boldsymbol{x}}\varphi(\boldsymbol{s},\boldsymbol{x}))&:\ \eta\in\mathrm{WF}_{(\boldsymbol{s},t)}(\mathbb{1}_A),\ \omega\in\dot{\mathbb{R}},\\ &\eta_n+\omega\neq0,\ \boldsymbol{x}\in\mathcal{I}(\boldsymbol{s},t),\exists\boldsymbol{x}_0\in\mathcal{X}(\boldsymbol{s},t,u),\\ &\mathrm{d}_{\boldsymbol{s}}\varphi(\boldsymbol{s},\boldsymbol{x})=\frac{1}{\eta_n+\omega}(\omega\,\mathrm{d}_{\boldsymbol{s}}\varphi(\boldsymbol{s},\boldsymbol{x}_0)-\eta')\big\}.\end{aligned} \tag{73}$$

Proof. We start with an arbitrary covector in $M^{\mathrm{nc}}(A,u)$,

$$\begin{gathered}(\boldsymbol{s},t,\eta'-\omega\,\mathrm{d}_{\boldsymbol{s}}(\boldsymbol{s},\boldsymbol{x}_0),\eta_n+\omega)\\ \text{where } (\boldsymbol{s},t)\in B_2^{\mathrm{nc}},\ \eta\in \mathrm{WF}_{(\boldsymbol{s},t)}(\mathbb{1}_A),\ \boldsymbol{x}_0\in\mathcal{X}(\boldsymbol{s},t,u),\ \omega\in\dot{\mathbb{R}}.\end{gathered}\tag{74}$$

The arbitrary covector in $\mathcal{C}_A^\top$ is

$$(\boldsymbol{x},\omega'\,\mathrm{d}_{\boldsymbol{x}}\varphi(\boldsymbol{s}',\boldsymbol{x});\boldsymbol{s}',t',-\omega'\,\mathrm{d}_{\boldsymbol{s}}\varphi(\boldsymbol{s},'\boldsymbol{x}),\omega')$$

where $(\boldsymbol{s}',t')\in A,\ \omega'\in\dot{\mathbb{R}},\ \boldsymbol{x}\in\mathcal{I}(\boldsymbol{s}',t')$, see (70). Equating the coefficients of the $T^*(Y)$ component of this covector with the covector in (74), we see $\boldsymbol{s}'=\boldsymbol{s},\ t'=t,\ \omega'=\eta_n+\omega\in\dot{\mathbb{R}}$, and

$$(\eta_n+\omega)\,\mathrm{d}_{\boldsymbol{s}}\varphi(\boldsymbol{s},\boldsymbol{x})=-\eta'+\omega\,\mathrm{d}_{\boldsymbol{s}}\varphi(\boldsymbol{s},\boldsymbol{x}_0).\tag{75}$$

Solving for $\mathrm{d}_{\boldsymbol{s}}\varphi(\boldsymbol{s},\boldsymbol{x})$, we get the final condition in (73). □

Remark C.4. *Assume $X\subset\mathbb{R}^2$. Let $(\boldsymbol{s},t)\in B_2^{\mathrm{nc}}$. Then we claim $M^{\mathrm{nc}}(A,u)\cap T^*_{(\boldsymbol{s},t)}(Y)$ contains all but at most two one-dimensional subspaces. This makes calculations of $\mathcal{C}_A^\top\circ M^{\mathrm{c}}(A,u)$ and $\mathcal{C}_A^\top\circ M^{\mathrm{nc}}(A,u)$ easier as will be described at the end of this remark.*

First, consider the case when $\mathrm{WF}_{(\boldsymbol{s},t)}(\mathbb{1}_A)$ is spanned by one covector η and $\mathrm{WF}_{(\boldsymbol{s},t)}(Fu)$ is spanned by one covector ν. Since $(\boldsymbol{s},t)\in B_2^{\mathrm{nc}}$, η and ν are independent, and linear combinations $\omega_1\eta+\omega_2\nu$ for $\omega_1\in\dot{\mathbb{R}}$ and $\omega_2\in\dot{\mathbb{R}}$ spans all but two one-dimensional subspaces of $T^*_{(\boldsymbol{s},t)}(Y)$, those spanned by η and by ν. If there are more independent covectors in either $\mathrm{WF}_{(\boldsymbol{s},t)}(\mathbb{1}_A)$ or $\mathrm{WF}_{(\boldsymbol{s},t)}(Fu)$, then all (or all but one) one-dimensional subspaces of $T^*_{(\boldsymbol{s},t)}(Y)$ are covered by this span.

Then, by an argument similar to the calculation in (71) in the proof of Proposition C.2, $\dot{N}^*(\mathcal{I}(\boldsymbol{s},t))$ is covered, except above at most two points in $\mathcal{I}(\boldsymbol{s},t)$, those corresponding to the two one-dimensional subspaces that are not covered by $M^{\mathrm{nc}}(A,u)\cap T^*_{(\boldsymbol{s},t)}(Y)$. Note that the uncovered subspaces are of the form $\omega_1\eta$, and $(\boldsymbol{s},t,\omega_1\eta)\in\mathrm{WF}(\mathbb{1}_A)$ and $(\boldsymbol{s},t,\omega_2\nu)\in\mathrm{WF}(Fu)$ so

$$S_{(\boldsymbol{s},t)}=\big(M^{\mathrm{nc}}(A,u)\cup M^{\mathrm{c}}(A,u)\cup\mathrm{WF}(\mathbb{1}_A)\cup\mathrm{WF}(Fu)\big)\cap T^*_{(\boldsymbol{s},t)}(Y)\tag{76}$$

contains all singularities above $(\boldsymbol{s},t)$. Note that this occurred in the limited data problem for the function $\mathbb{1}_{I^2}$ in Section 4.2 on the line $\mathcal{I}(\pi/2,2/3)$.

This means that, in the two-dimensional case, to find singularities of $\mathbb{1}_AFu$ above $(\boldsymbol{s},t)\in B_2$, one can take all singularities, and they will be in $S_{(\boldsymbol{s},t)}$.

Therefore, all singularities in $\dot{N}^*(\mathcal{I}(\boldsymbol{s},t))$ are in the union in (37). Note that this does not mean that all these singularities are in $\mathcal{L}u$, but they will be if F and F^* satisfy the Bolker condition.

Remark C.5. *We now explain how object dependent and object independent singularities can be generated by singularities above the same point in $\mathrm{Bd}(A)$.*

We recall the notation of Section 4.2. Let Ω be the open unit disk in $\mathbb{R}^2$ and let R be the Radon line transform. For $(s,t)\in[0,\pi]\times(-1,1)$ let $\mathcal{I}(s,t)$ be the line perpendicular to $\Theta(s)$ and containing $t\Theta(s)$. Then, $Ru(s,t)$ is the integral of u over $\mathcal{I}(s,t)$. The limited data set is $A=[0,\pi]\times[-2/3,2/3]$.

As calculated in (51), the following singularities are in $\mathcal{C}_A^\top\circ M^{\mathrm{nc}}(A(2/3),u)$

$$\big\{(\boldsymbol{x},0,1):\ \boldsymbol{x}\in\mathcal{I}(\pi/2,2/3)\setminus\{(0,2/3)\}\big\}.$$

As can be seen from (53),

$$(0,2/3,0,1)\in\mathcal{C}_A^\top\circ\mathrm{WF}_{\mathrm{supp}(Fu)}(\mathbb{1}_A),$$

and this is an object independent singularity since it does not depend on the singularities of u.

Putting this together, we see that $(\pi/2, 2/3)$ generates both object dependent and object independent singularities. Figure 3 seems to show all these singularities.

Acknowledgment: The authors thank Kevin Ganster for kindly providing the reconstructions displayed in Section 4.3 using his code published in [14]. The first author thanks John Schotland and Guillaume Bal for a conversation on multiplying functions that inspired this line of research.

REFERENCES

[1] A. ABHISHEK, A. KATSEVICH, AND J. W. WEBBER, *Statistical microlocal analysis in two-dimensional X-ray CT*, Inverse Problems, 41 (2025), pp. Paper No. 125001, 28, https://doi.org/10.1088/1361-6420/ae2290.

[2] M. L. AGRANOVSKY AND E. T. QUINTO, *Injectivity sets for the Radon transform over circles and complete systems of radial functions*, J. Funct. Anal., 139 (1996), pp. 383–414, https://doi.org/10.1006/jfan.1996.0090.

[3] G. AMBARTSOUMIAN, R. FELEA, V. P. KRISHNAN, C. J. NOLAN, AND E. T. QUINTO, *Singular FIOs in SAR imaging, II: Transmitter and receiver at different speeds*, SIAM J. Math. Anal., 50 (2018), pp. 591–621, https://doi.org/10.1137/17M1125741.

[4] G. AMBARTSOUMIAN, R. FELEA, V. P. KRISHNAN, C. J. NOLAN, AND E. T. QUINTO, *Microlocal analysis of Radon transforms over quadric surfaces*, 2026, https://arxiv.org/abs/2602.12453. Submitted February 2026.

[5] H. ANDRADE-LOARCA, G. KUTYNIOK, O. ÖKTEM, AND P. PETERSEN, *Deep microlocal reconstruction for limited-angle tomography*, Appl. Comput. Harmon. Anal., 59 (2022), pp. 155–197, https://doi.org/10.1016/j.acha.2021.12.007.

[6] N. BLEISTEIN, J. K. COHEN, AND J. W. STOCKWELL, JR., *Mathematics of multidimensional seismic imaging, migration, and inversion*, vol. 13 of Interdisciplinary Applied Mathematics, Springer-Verlag, New York, 2001, http://dx.doi.org/10.1007/978-1-4613-0001-4. Geophysics and Planetary Sciences.

[7] L. BORG, J. FRIKEL, J. S. JØRGENSEN, AND E. T. QUINTO, *Analyzing reconstruction artifacts from arbitrary incomplete X-ray CT data*, SIAM J. Imaging Sci., 11 (2018), pp. 2786–2814, https://doi.org/10.1137/18M1166833.

[8] T. A. BUBBA, G. KUTYNIOK, M. LASSAS, M. MÄRZ, W. SAMEK, S. SILTANEN, AND V. SRINIVASAN, *Learning the invisible: a hybrid deep learning–shearlet framework for limited angle computed tomography*, Inverse Problems, 35 (2019), pp. 064002, 38, https://doi.org/10.1088/1361-6420/ab10ca.

[9] R. FELEA, V. P. KRISHNAN, C. J. NOLAN, AND E. T. QUINTO, *Common midpoint versus common offset acquisition geometry in seismic imaging*, Inverse Probl. Imaging, 10 (2016), pp. 87–102, https://doi.org/10.3934/ipi.2016.10.87.

[10] R. FELEA AND E. T. QUINTO, *The microlocal properties of the local 3-D SPECT operator*, SIAM J. Math. Anal., 43 (2011), pp. 1145–1157, https://doi.org/10.1137/100807703.

[11] J. FRIKEL AND E. QUINTO, *Characterization and reduction of artifacts in limited angle tomography*, Inverse Problems, 29 (2013), pp. 125007, 21, http://dx.doi.org/10.1088/0266-5611/29/12/125007.

[12] J. FRIKEL AND E. T. QUINTO, *Artifacts in incomplete data tomography with applications to photoacoustic tomography and sonar*, SIAM J. Appl. Math., 75 (2015), pp. 703–725, https://doi.org/10.1137/140977709.

[13] J. FRIKEL AND E. T. QUINTO, *Limited data problems for the generalized Radon transform in $\mathbb{R}^n$*, SIAM J. Math. Anal., 48 (2016), pp. 2301–2318, https://doi.org/10.1137/15M1045405.

[14] K. GANSTER, *A microlocal and visual comparison of 2D Kirchhoff migration formulas - software package*, 2024, https://dx.doi.org/10.35097/YeHLCWQEafknUBDA.

[15] K. GANSTER, E. T. QUINTO, AND A. RIEDER, *A microlocal and visual comparison of 2D Kirchhoff migration formulas in seismic imaging*, Inverse Problems, 40 (2024), pp. Paper No. 115001, 29, https://doi.org/10.1088/1361-6420/ad797b.

[16] K. GANSTER AND A. RIEDER, *Approximate Inversion of a Class of Generalized Radon Transforms*, SIAM J. Imaging Sci., 16 (2023), pp. 842–866, https://doi.org/10.1137/22M1512417.
[17] C. GRATHWOHL, P. KUNSTMANN, E. T. QUINTO, AND A. RIEDER, *Microlocal analysis of imaging operators for effective common offset seismic reconstruction*, Inverse Problems, 34 (2018), pp. 114001, 24, https://doi.org/10.1088/1361-6420/aadc2a.
[18] A. GREENLEAF AND G. UHLMANN, *Nonlocal inversion formulas for the X-ray transform*, Duke Math. J., 58 (1989), pp. 205–240, https://doi.org/10.1215/S0012-7094-89-05811-0.
[19] V. GUILLEMIN, *On some results of Gel'fand in integral geometry*, in Pseudodifferential operators and applications (Notre Dame, Ind., 1984), vol. 43 of Proc. Sympos. Pure Math., Amer. Math. Soc., Providence, RI, 1985, pp. 149–155, https://doi.org/10.1090/pspum/043/812288.
[20] V. GUILLEMIN AND S. STERNBERG, *Geometric asymptotics*, American Mathematical Society, Providence, R.I., 1977. Mathematical Surveys, No. 14.
[21] B. N. HAHN AND E. T. QUINTO, *Detectable singularities from dynamic Radon data*, SIAM J. Imaging Sci., 9 (2016), pp. 1195–1225, https://doi.org/10.1137/16M1057917.
[22] C. HAMAKER, K. T. SMITH, D. C. SOLMON, AND S. L. WAGNER, *The divergent beam X-ray transform*, Rocky Mountain J. Math., 10 (1980), pp. 253–283, https://doi.org/10.1216/RMJ-1980-10-1-253.
[23] L. HÖRMANDER, *Fourier integral operators. I*, Acta Math., 127 (1971), pp. 79–183, http://link.springer.com/article/10.1007/BF02392052.
[24] L. HÖRMANDER, *The analysis of linear partial differential operators I: Distribution theory and Fourier analysis*, Classics in Mathematics, Springer-Verlag, Berlin, 2003, https://doi.org/10.1007/978-3-642-61497-2.
[25] L. HÖRMANDER, *The analysis of linear partial differential operators. IV*, Classics in Mathematics, Springer-Verlag, Berlin, 2009, https://doi.org/10.1007/978-3-642-00136-9. Fourier integral operators, Reprint of the 1994 edition.
[26] A. I. KATSEVICH, *Local tomography for the limited-angle problem*, J. Math. Anal. Appl., 213 (1997), pp. 160–182, https://doi.org/10.1006/jmaa.1997.5412.
[27] P. KUCHMENT AND L. KUNYANSKY, *Mathematics of thermoacoustic tomography*, European J. Appl. Math., 19 (2008), pp. 191–224, https://doi.org/10.1017/S0956792508007353.
[28] P. C. KUNSTMANN, E. T. QUINTO, AND A. RIEDER, *Seismic imaging with generalized Radon transforms: stability of the Bolker condition*, Pure Appl. Math. Q., 19 (2023), p. 1985–2036, https://dx.doi.org/10.4310/PAMQ.2023.v19.n4.a11.
[29] H. LEVINSON, *Reconstruction algorithms for bistatic radar and ultrasound imaging*, Bachelor's Thesis, Tufts Archival Research Center, Tufts University, 2011, http://hdl.handle.net/10427/71452.
[30] A. K. LOUIS, *Picture reconstruction from projections in restricted range*, Math. Methods Appl. Sci., 2 (1980), pp. 209–220, https://doi.org/10.1002/mma.1670020207.
[31] A. K. LOUIS AND E. T. QUINTO, *Local tomographic methods in sonar*, in Surveys on solution methods for inverse problems, Springer, Vienna, 2000, pp. 147–154.
[32] A. K. LOUIS AND A. RIEDER, *Incomplete data problems in X-ray computerized tomography. II. Truncated projections and region-of-interest tomography*, Numer. Math., 56 (1989), pp. 371–383, https://doi.org/10.1007/BF01396611.
[33] F. NATTERER, *The mathematics of computerized tomography*, vol. 32 of Classics in Applied Mathematics, Society for Industrial and Applied Mathematics (SIAM), Philadelphia, PA, 2001, http://dx.doi.org/10.1137/1.9780898719284. Reprint of the 1986 original.
[34] L. V. NGUYEN, *How strong are streak artifacts in limited angle computed tomography?*, Inverse Problems, 31 (2015), pp. 055003, 26, https://doi.org/10.1088/0266-5611/31/5/055003.
[35] L. V. NGUYEN AND T. A. PHAM, *Microlocal analysis for spherical Radon transform: two nonstandard problems*, Inverse Problems, 35 (2019), pp. 074001, 15, https://doi.org/10.1088/1361-6420/ab15df.
[36] B. E. PETERSEN, *Introduction to the Fourier transform and pseudo-differential operators*, vol. 19 of Monographs and Studies in Mathematics, Pitman (Advanced Publishing Program), Boston, MA, 1983.
[37] J. QIAN AND W. W. SYMES, *An adaptive finite-difference method for traveltimes and amplitudes*, Geophysics, 67 (2002), p. 167, https://doi.org/10.1190/1.1451472.
[38] E. T. QUINTO, *Singularities of the X-ray transform and limited data tomography in* $\mathbf{R}^2$ *and* $\mathbf{R}^3$, SIAM J. Math. Anal., 24 (1993), pp. 1215–1225, https://doi.org/10.1137/0524069.

[39] E. T. QUINTO, T. BAKHOS, AND S. CHUNG, *Local tomography in 3-D SPECT*, in Mathematical methods in biomedical imaging and intensity-modulated radiation therapy (IMRT), vol. 7 of CRM Series, Ed. Norm., Pisa, 2008, pp. 321–348.

[40] A. RIEDER AND A. FARIDANI, *The semidiscrete filtered backprojection algorithm is optimal for tomographic inversion*, SIAM J. Numer. Anal., 41 (2003), pp. 869–892 (electronic), http://dx.doi.org/10.1137/S0036142902405643.

[41] M. ROSENBLATT, M. MORVIDONE, AND J. CEBEIRO, *Microlocal properties of the Radon transform on V-lines: a framework to reduce artifacts due to intrinsic missing data in linear Compton cameras*, Inverse Problems, 41 (2025), pp. Paper No. 035004, 27, https://doi.org/10.1088/1361-6420/adb2bb.

[42] W. RUDIN, *Functional analysis*, McGraw-Hill Book Co., New York-Düsseldorf-Johannesburg, 1973. McGraw-Hill Series in Higher Mathematics.

[43] P. STEFANOV, *The Radon transform with finitely many angles*, Inverse Problems, 39 (2023), pp. Paper No. 105003, 34, https://doi.org/10.1088/1361-6420/acef53.

[44] W. W. SYMES, *Mathematics of reflection seismology*, tech. report, The Rice Inversion Project, Rice University, Houston, TX, USA, 1998, http://www.trip.caam.rice.edu/downloads/preamble.pdf.

[45] F. TERZIOGLU, *Some analytic properties of the cone transform*, Inverse Problems, 35 (2019), pp. 034002, 22, https://doi.org/10.1088/1361-6420/aafccf.

[46] F. TRÈVES, *Introduction to pseudodifferential and Fourier integral operators. Vol. 1*, Plenum Press, New York-London, 1980. Pseudodifferential operators, The University Series in Mathematics.

[47] F. TRÈVES, *Introduction to pseudodifferential and Fourier integral operators. Vol. 2*, Plenum Press, New York-London, 1980. Fourier integral operators, The University Series in Mathematics.

[48] Y. WANG, *Identification of nonlinear beam-hardening effects in X-ray tomography*, SIAM J. Math. Anal., 56 (2024), pp. 7290–7305, https://doi.org/10.1137/23M1596491.

[49] J. W. WEBBER AND S. HOLMAN, *Microlocal analysis of non-linear operators arising in Compton CT*, Inverse Problems, 42 (2026), pp. Paper No. 025007, 24, https://doi.org/10.1088/1361-6420/ae3acc.

[50] J. W. WEBBER AND E. T. QUINTO, *Spherical radon transforms with smoothly varying radii*, 2026, https://doi.org/10.48550/arXiv.2602.23512. submitted, February, 2026.